



**PennState**  
College of Engineering



# ESM TODAY 2022

February 26, 2022  
1<sup>st</sup> Floor Lobby EES Building

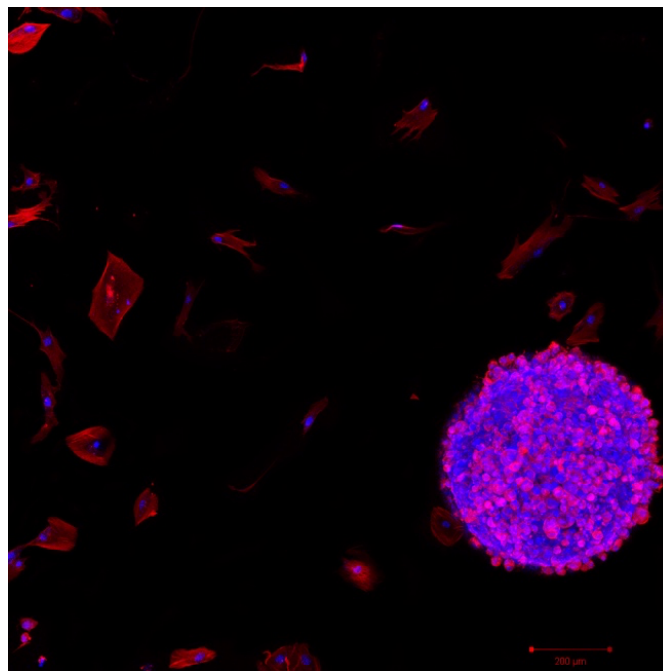


*Photo courtesy of Nazmiye Celik, 2021 ESM Today Art-in-Science Winner*

19<sup>th</sup> Annual Engineering Science and  
Mechanics Research Symposium

# Table of Contents

Schedule of Events	3
Keynote Speaker	4
Participants Lists and Abstract Titles	5
Oral Presentations	8
Poster Presentations	46
Art-in-Science	58

**ESM Today 2022 organized by:**

Nailah Oliver

Olivia Cook

Rahul Pendurthi

Shiva Subbulakshmi Radhakrishnan

## Schedule of Events

<b>8:00 AM – 8:30 AM</b>	<b>Breakfast and Registration</b>
<b>8:30 AM – 8:45 AM</b>	<b>Introduction by Dr. Todd</b>
<b>8:45 AM – 9:15 AM</b>	<b>Keynote Speaker: Doug Evans</b>
<b>9:15 AM – 9:30 AM</b>	<b>Break</b>
<b>9:30 AM – 12:00 PM</b>	<b>Oral Presentations Rooms 114, 116, 119, and 121</b>
<b>12:00 PM – 1:45 PM</b>	<b>Poster Presentations &amp; Art-in- Science Exhibition</b>
<b>1:45 PM – 2:30 PM</b>	<b>Safety Olympics</b>
<b>2:30 PM – 3:00 PM</b>	<b>Awards Ceremony</b>

## Keynote Speaker

**Doug Evans**

*Distinguished ESM Alumni*



**Zoom Link for Virtual Participants:**

<https://psu.zoom.us/j/99891437386>

Doug Evans, P.E. graduated with a B.S. in Engineering Science with Honors in Bioengineering from Penn State University in 1986 and a M.S. in Electrical Engineering (1989) and Business Management (1993) from University of Pennsylvania and Penn State respectively. He is the President & CEO of Lungpacer Medical Inc., which is developing AeroPace™, a novel therapeutic neurostimulation technology to power natural breathing for patients by preserving the integrity and strength of the diaphragm muscle, and by providing lung and brain protection for critically ill patients who require artificial ventilation, a US \$10 billion market opportunity. He is an accomplished medical device executive, business leader, and strategist with 30 years of industry, public, and private company experience. He is a serial innovator of first-of-their-kind products, such as the Angio-Seal Vascular Closure Device and the AeroPace Therapy System, has 96 issued US patents covering dozens of devices, which have been used in over 15 million patients world-wide and generated greater than \$4 billion in end-user sales, and 12 publications. He was recognized as one of 100 notable in the Medical Device Industry by MD&DI magazine for significant contributions to the medical device industry.

Doug Evans is also the co-founder of Cure4Cam Childhood Cancer Foundation, which seeks to raise community awareness about childhood cancers and supports the development of new and more humane therapies for children with these diseases.

# Participants Lists and Abstract Titles

Oral Presentations			
Speaker	Abstract Title	Speaker	Abstract Title
<b>Waves, Acoustics, and Ultrasonics</b>			
Caeden Smith	<i>Noninvasive Tracking of Solidification Using Ultrasound</i>	Colin Williams	<i>Utilizing Nonlinear Ultrasonic Methods for the Characterization of Mechanical Properties in Additively Manufactured Components</i>
Fedor Viktorovich Sharov	<i>An Electrically Detected Near-Adiabatic Rapid-Sweep Approach to Electrically Detected Magnetic Resonance and Near-Zero-Field Magnetoresistance</i>	Lalith Sai Srinivas Pillarisetti	<i>Control of low-frequency axisymmetric longitudinal and torsional guided wave modes in a hollow pipe using a meta-surface</i>
Linying Gao	<i>The effect of grain angularity and relative humidity on the nonlinear elastic response of granular media</i>	Prabhakaran Manogharn	<i>Development of In-situ Dynamic Acoustoelastic Testing Using a Thermal Strain Pump</i>
Prabhav Borate*	<i>Shear failure prediction from active source ultrasonic data using deep learning frameworks</i>	Evan Bozek	<i>Contact and Non-Contact Characterization of Additively Manufactured and Wrought Samples</i>
<b>2D Materials and MEMS/NEMS Devices</b>			
Aaryan Oberoi	<i>Bottom-up Implementation of Hardware Security primitives on 2D Materials</i>	Avery Brown	<i>Tension-Tension Fatigue Behavior of Carbon/Epoxy Composites with Concentrated Carbon Nanotube Interlayers for High Damping</i>
Faheem Ershad	<i>Drawn-on-Skin Bioelectronics for Motion Artifact-Free Sensing and Point-of-Care Treatment</i>	Henry Dyer	<i>Dynamic Mechanical Behavior of Carbon Nanotube Yarns</i>

\*Multiple specialty areas are associated with the presentation.

Oguzhan Colak	Untitled	Stephen Moxim*	<i>Tracking atomic-scale defects involved in metal-oxide-semiconductor device stressing with simple near-zero-field magnetoresistance measurements</i>
Yongwen Sun	<i>Stacking fault (SF) mapping by 4DSTEM</i>		
<b>Machine Learning</b>			
Akhil Dodda	<i>A Low-Power, Bio-inspired, Adaptive Machine Vision Sensor based on Atomically Thin Memtransistors</i>	Christopher Wheatley Jr (Zoom)	<i>Algorithm for Grain Size Analysis and Phase Segmentation (AGAPS)</i>
Dipanjan Sen	<i>A Sparse and Spike-timing based Adaptive Photo Encoder for Augmenting Machine Vision for Spiking Neural Networks</i>	Ferris Arnous	<i>Application of Multidomain Image Data Fusion For Enhanced Convolutional Neural Network Classification</i>
Harikrishnan Ravichandran	<i>A Monolithic Stochastic Computing Architecture for Energy Efficient Arithmetic Enabled by 2D Memtransistors</i>	Mayukh Das*	<i>A Robust Insect Inspired Spike-Based Collision Detector</i>
Shiva Subbulakshmi Radhakrishnan	<i>An All-in-One 2D Neuromorphic System</i>	Andrew Pannone*	<i>In-Memory Gaussian Synapses based on 2D CMOS FETs</i>
<b>Life Sciences and Chemistry</b>			
Adam Alavi	<i>Proton Conductivity in Squid Ting Teeth Protein Membrane</i>	Farshad Ghanbari	<i>Modeling Fungal Infections: Matrix Development in Zombie Ants</i>
Myoung Hwan Kim	<i>Aspiration-assisted freeform bioprinting of mesenchymal stem cell spheroids within alginate microgels</i>	Nazmiye Celik	<i>miRNA Induced 3D Bioprinted-Heterotypic Osteochondral Interface</i>

\*Multiple specialty areas are associated with the presentation.

<b>Mechanics of Materials and Additive Manufacturing</b>			
Arnab Chatterjee	<i>Additive Manufacturing build plan dependence of spatially resolved structure-behavior relations in active materials</i>	Clay Wood	<i>Probing the Micromechanical Features of a Fracture Interface Using a Multi-Physics Approach: A Numerical Investigation Relating Asperity Deformation with Fluid Flow</i>
Lauren Katch*	<i>Ultrasonic scattering from subwavelength cracks in anisotropic silicon</i>	Mecit Altan Alioglu	Untitled
Michail Skiadopoulos	<i>Digital Translation of Micrographs for Finite Element Modelling of Mechanical Response</i>	Raghul Asokkumar	<i>A Comparative Study of Directed Energy Deposition (DED) and Powder Bed Fusion (PBF) Parts Using 316L Stainless Steel Powders</i>

<b>Poster Presentations</b>			
<b>Speaker</b>	<b>Abstract Title</b>	<b>Speaker</b>	<b>Abstract Title</b>
Aaryan Oberoi	<i>Bottom-up Implementation of Hardware Security primitives on 2D Materials</i>	Abhirup Saha	<i>Identifying Mechanisms for Eliminating Defects during the Laser Welding of Aluminum Alloys</i>
Arnab Chatterjee	<i>Spatial characterization approach for understanding Fabrication-Microstructure-Property relationships of Titanium rich LDED based Nitinol along overlap of passes and layers interfaces</i>	Clay Wood	<i>Relating fracture aperture to hydro-mechanical properties of dynamically stressed tensile fractured rock</i>
Faheem Ershad	<i>Drawn-on-Skin Bioelectronics for Motion Artifact-Free Sensing and Point-of-Care Treatment</i>	Nazmiye Celik	<i>miRNA Induced 3D Bioprinted-Heterotypic Osteochondral Interface</i>
Rahul Pendurthi	<i>Monolithic and Heterogeneous Integration of Atomically Thin Transition Metal Dichalcogenides for non von Neumann CMOS</i>	Yikai Zheng	<i>Hardware Acceleration of Bayesian Network based on Two-dimensional Memtransistors</i>

\*Multiple specialty areas are associated with the presentation.

# Oral Presentations

## List of Speakers and Judges

Time	114 EES Zoom link: <a href="https://psu.zoom.us/j/99891437386">https://psu.zoom.us/j/99891437386</a>	116 EES Zoom link: <a href="https://psu.zoom.us/j/94767395884">https://psu.zoom.us/j/94767395884</a>	119 EES Zoom link: <a href="https://psu.zoom.us/j/99489488554">https://psu.zoom.us/j/99489488554</a>	121 EES Zoom link: <a href="https://psu.zoom.us/j/91228050628">https://psu.zoom.us/j/91228050628</a>
	Presenters			
9:30 AM – 9:45 AM	Evan Bozek	Colin Williams	Fedor Viktorovich Sharov	Lalith Sai Srinivas Pillarisetti
9:45 AM – 10:00 AM	Aaryan Oberoi	Henry Dyer	Faheem Ershad	Avery Brown
10:00 AM – 10:15 AM	Adam Alavi	Farshad Ghanbari	Myoung Hwan Kim	Nazmiye Celik
10:15 AM – 10:30 AM	Arnab Chatterjee	Christopher Wheatley Jr	Lauren Katch	Mecit Altan Alioglu
10:30 AM – 10:45 AM	Akhil Dodda	Shiva Subbulakshmi Radhakrishnan	Mayukh Das	Ferris Arnous
10:45 AM – 11:00 AM	<b>Break</b>			
11:00 AM – 11:15 AM	Linying Gao	Prabhakaran Manogharn	Caeden Smith	Prabhav Borate
11:15 AM – 11:30 AM	Oguzhan Colak	Stephen Moxim	Raghul Asokkumar	Yongwen Sun
11:30 AM – 11:45 AM	Harikrishnan Ravichandran	Dipanjan Sen	Andrew Pannone	Clay Wood
11:45 AM – 12:00 PM				Michail Skiadopoulos
<b>Judges</b>	<b>Faculty</b>			
	Al Segall	Akhlesh Lakhtakia	Jacques Riviere	Saptarshi Das
	Andrew Geronimo	Elizabeth Sikora	Robert W. Smith	Andrea Arguelles
	<b>Students</b>			
	Suparno Bhattacharyya	Tanner Sherry	Xinyi Li	Irem Derman
Vaibhav Pal	Foster Feni	Nailah Oliver	Rahul Pendurthi	

## **Noninvasive Tracking of Solidification Using Ultrasound**

*Caeden Smith*

Noninvasive tracking of solidification is typically done by monitoring the sample's surface temperature. This approach is error-prone and not always appropriate for complex geometries and often does not provide complete information on the sample's transitioning phases. This feasibility study investigates using ultrasonic waves to noninvasively track solidification in wax. Ultrasonic sensors are used in through-transmission mode to monitor the response over the solidification period. The difference in speed of sound between the wax's liquid and solid phase allowed for the time of complete solidification to be identified. Temperature probes are used to verify the results obtained from the ultrasonic data. The ultimate goal of the project is to use a metal sample and connect information from the ultrasonic signal to the material properties and grain structure of the cast using noninvasive ultrasound technology.

## **Utilizing Nonlinear Ultrasonic Methods for the Characterization of Mechanical Properties in Additively Manufactured Components**

*Colin Williams*

The ultimate goal of this research is to find new noninvasive methods to certify the quality of safety-critical additively manufactured (AM) metallic parts for use in industries such as aerospace and defense. Additive manufacturing facilitates rapid prototyping, repairing, and building of custom components with increased agility, production rate, and reduced waste. A recognized barrier to the wide adoption of AM is the lack of new approaches for AM part qualification. Our research objective is to exploit the material's linear and nonlinear ultrasonic response - which represents the measurable changes and distortion in elastic waves encountering macroscopic and microscopic defects - to establish links between microstructure and macro-scale elastic properties of AM metals.

Using the nonlinear ultrasonic method of Second Harmonic Generation (SHG), the acoustic nonlinearity parameter is estimated in a series of 316-grade stainless steel samples of varying heat treatments. For each heat treatment, a set of specimens is manufactured using AM methods, while a second set is manufactured using traditional wrought manufacturing. SHG has been shown to offer a highly sensitive response to microstructural heterogeneities within a material's microstructure, such as dislocations and grain boundaries. A linear ultrasonic parameter, wave speed, is also recorded. Alongside these ultrasonic measurements, mechanical testing parameters including elastic moduli and yield strength are evaluated for the specimens.

Results indicate correlations between the nonlinearity parameter and both ultimate tensile strength and yield strength, where nonlinearity generally decreases as these mechanical parameters increase, particularly in the AM samples. We hypothesize that microstructural changes in grain size and distribution through the heat treatment process influences these trends in measured nonlinearity. These results show promising evidence for the feasibility of AM part qualification using nondestructive ultrasonic testing. Future work includes continuing SHG testing, as well as comparing SHG results to different nonlinear ultrasonic methods used to test these samples. Further, the microstructures will be imaged using electron microscopy to evaluate our hypothesis, and fundamental numerical simulations will be conducted to better understand the effects of heterogeneity on the material's nonlinear response.

# An Electrically Detected Near-Adiabatic Rapid-Sweep Approach to Electrically Detected Magnetic Resonance and Near-Zero-Field Magnetoresistance

*Fedor Sharov, Advised by Dr. Patrick Lenahan*

Electrically detected magnetic resonance (EDMR) is a powerful analytical spectroscopic tool that allows for the chemical identification of atomic-scale defects. However, the long acquisition times make analysis of real-time effects difficult to observe in the spectra. In this paper, we demonstrate a new method for accumulating spectra using near-adiabatic rapid-sweep (NARS) [1] methodology to observe spin-dependent trap assisted tunneling (SDTAT) through -Si:H capacitor dots and spin-dependent recombination (SDR) in 4H-SiC MOSFETs. This technique shows promise in significantly increasing the signal-to-noise ratios of the EDMR spectra of many device systems with superior time-scale resolution.

In continuous-wave (CW) EDMR, devices are placed within a resonant cavity tuned to a certain resonant frequency stationed within a large slow-sweeping electromagnet. A secondary high-frequency sweep is provided by a set of modulation coils typically operating around 1 kHz. While this set-up provides high sensitivity, the timescales involved with each scan are long, and the lock-in detection is susceptible to  $1/f$  noise of the measurements.

We have developed a new apparatus for electrically detected rapid-scan measurements based on rapid-scan EPR (RSEPR) [2]. In this set-up, the central magnetic field is held constant at or around resonance, as the modulation coils provide triangular sweeps through resonance at high frequency. We present X-band data showing NARS EDMR spectra that are undistorted and identical to both SDTAT and SDR CW-EDMR spectra that are less susceptible to  $1/f$  noise. This experimental set-up preserves the CW-EDMR line shape and chemical information, while providing a boost in sensitivity and time-resolution, with few changes to the experimental apparatus.

Additionally, we use this set-up to detect SDTAT via near-zero-field magnetoresistance (NZFMR). NZFMR has been modeled using the stochastic quantum Liouville equation (SQLE) [3] to define a steady-state solution for traditional slow-sweep NZFMR experiments. This approach has been used to identify important chemical devices in semiconductor devices, such as nuclear hyperfine constants and kinetic rates.

In the case of NZFMR, there is no radio-frequency microwave radiation that sets the resonant field or supplies power to the system. Thus, the non-equilibrium interactions occurring at higher frequencies are due solely to spin-mixing near-zero fields. Using this apparatus, we can observe non-equilibrium effects in the NZFMR line shape. Further analysis of non-steady state solutions to the SQLE predict similar trends to what is observed with this electrically detected rapid-scan apparatus as the rate at which the magnetic field is swept is increased. These results suggest that rapid-scan methodology can be applied to EDMR and NZFMR in a similar manner to RSEPR to garner increases in sensitivity, inspect non-equilibrium defect interactions, and higher resolution of time-dependent device physics.

## References

- [1] Kittell, A. W. et al, J. Magn. Reson. 211, 228–233 (2011).
- [2] Quine, R. W. et al., J. Magn. Reson. 205, 23–27 (2010).
- [3] Frantz, E. B. et al., J. Appl. Phys. 130, (2021).

## **Control of low-frequency axisymmetric longitudinal and torsional guided wave modes in a hollow pipe using a meta-surface**

*Lalith Sai Srinivas Pillarisetti*

Ultrasonic guided wave inspection is the most commonly used technique for assessing the structural integrity of hollow pipes due to the ability of guided waves to travel longer distances. Among numerous possible dispersive guided modes, the low-frequency longitudinal modes  $L(0,1)$  and  $L(0,2)$ , and the torsional mode ( $T(0,1)$ ), are widely used for pipeline inspections. The proposed study aims to control these guided modes using a locally resonant metasurface for applications towards improving the nonlinear ultrasonic measurements and reducing the complexity of the transducer configuration to preferentially excite the  $L(0,2)$  guided mode over the  $L(0,1)$ . The former application requires complete suppression of all the guided wave modes ("complete" bandgap), whereas the latter requires preferential transmission of a specific longitudinal guided wave mode ("partial" bandgap). The proposed metamaterial comprises a circular array of prismatic resonators bonded in a periodic arrangement along the axis of the pipe. The eigenfrequency analysis on a unit cell comprising the pipe and resonator indicates the presence of complete bandgaps for  $L(0,1)$ ,  $L(0,2)$ , and  $T(0,1)$  modes. Moreover, we obtain a partial bandgap where  $L(0,2)$  mode can be preferentially transmitted over  $L(0,1)$ . Time-domain finite element analysis is performed to validate the presence of these bandgaps by exciting different guided modes on the metasurface close to the bandgap frequencies. This work provides the first-ever insight into the capability of local resonant metamaterials to filter guided wave modes in hollow pipes, which can offer tremendous benefits to improve pipeline inspections.

# **The effect of grain angularity and relative humidity on the nonlinear elastic response of granular media**

*Linying Gao*

Nonlinear elastic effects arise in solids due to the presence of imperfections at the micro/mesoscopic scale, such as cracks or dislocations. Understanding the origins of these nonlinear elastic effects is critical to numerous fields, from geophysics and civil engineering to the non-destructive evaluation of materials. Elastic nonlinearity is particularly large in poorly consolidated or unconsolidated materials, where nonlinearity arises from weak junctions between grains. Previous work suggests that the nonlinear elastic response of consolidated granular media like rocks arises from two distinct mechanisms, one that might be related to the opening/closing of grain contacts, and the other one related to shearing of the grain junctions. To confirm this hypothesis and better understand the underlying physics, we seek to investigate the nonlinear elastic response of simpler systems (in terms of composition and microstructural features). First, we study the influence of relative humidity on the nonlinear elastic properties of glass bead samples. The changes in RH are used as a simple way to tweak the properties of the contact junctions and we find that the elastic nonlinearity of humid samples is an order of magnitude larger than that of dry samples. Moreover, we find that all extracted nonlinear parameters increase with RH. This suggests that, if indeed both mechanisms exist, they are affected in a similar fashion in these glass bead samples and cannot be distinguished using changes in RH. Second, we study the influence of grain shape on the nonlinear elastic properties of granular media. The elastic nonlinearity of angular grains made of fine quartz sand is compared with that of spherical glass beads. Our preliminary results suggest that the elastic nonlinearity of spherical and angular grains is of the same order of magnitude. However, the elastic nonlinearity of angular grains shows a much weaker dependence on RH changes than the spherical glass beads. These results suggest that unlike in glass beads, water adsorption is unable to weaken the contact junctions due to the locking of the angular grains. Finally, our preliminary results suggest that, unlike in spherical glass beads, not all nonlinear parameters behave in a similar fashion with changes in RH when the grains are angular. Taken together, we expect that this work will help us confirm our initial assumption that two main physical mechanisms exist, related to opening/closing and shearing of the grain junctions and/or microcracks.

## **Development of In-situ Dynamic Acoustoelastic Testing Using a Thermal Strain Pump**

*Prabhakaran Manogharan*

Dynamic acoustoelastic testing (DAET) is a pump-probe technique employed to measure the nonlinear elastic behavior of a test specimen. In DAET, the strain-induced changes in the wave speed and attenuation due to the low-frequency oscillation of the pump wave are measured by a high-frequency probe wave. DAET is comparable to the earlier quasi-static acoustoelastic experiments except that the stepwise load is replaced by a low-frequency stress/strain oscillation providing the ability to measure nonlinear elastic properties during both tension and compression phase of the pump strain. While DAET offers unprecedented information (classical and non-classical nonlinear features) about the nonlinear elastic response of materials, field applications of DAET are still challenging due to the need to apply a sufficiently strong strain pump. To facilitate the transition of DAET to in-situ evaluation, we propose a modification to the conventional DAET setup where we replace the mechanical strain pump with a thermal strain pump. This study investigates the feasibility of using thermal pump DAET setup to characterize surface-breaking cracks in an aluminum specimen. We use surface Rayleigh waves to probe the near-surface damage-induced nonlinearity. A hot blower is used to induce thermal strain across the crack surface while simultaneously thermal images are captured using an IR thermal camera to measure the strain produced in the sample. The relative velocity change in the Rayleigh wave with applied thermal strain is measured at various locations along the intact and cracked path. Our results show that the proposed DAET setup using a thermal pump can be potentially used in-situ to characterize surface-breaking cracks.

# Shear failure prediction from active source ultrasonic data using deep learning frameworks

*Borate, P.<sup>1</sup>, Girkar, V.<sup>2</sup>, Riviere, J.<sup>1</sup>, Kifer, D.<sup>2</sup>, Marone, C.<sup>3</sup>, Shokouhi, P.<sup>1</sup>*

<sup>1</sup> Engineering Science and Mechanics, Pennsylvania State University, University Park, PA, United States

<sup>2</sup> Department of Computer Science & Engineering, Pennsylvania State University, University Park, PA, United States

<sup>3</sup> Department of Geosciences, Pennsylvania State University, University Park, PA, United States

## Abstract

Prediction of micro-earthquakes when monitoring geothermal reservoirs, CO<sub>2</sub> storage sites, and unconventional reservoirs using active source seismic data although challenging, is essential to ensuring the safety of the operations. Laboratory-scale friction experiments have shown that changes in elastic wave amplitude and speed during active source monitoring carry precursory information about the upcoming failure. The friction experiment is conducted close to the stability boundary producing numerous regular and irregular seismic cycles. A pair of the P-wave ultrasonic transducer is used to probe the laboratory fault throughout the seismic cycles. The data-driven deep learning models predict the timing and size (shear stress drop) of the laboratory earthquakes with great accuracy using the elastic wave attributes (physics-based wave speed and amplitude).

In the active source ultrasonic monitoring, the ultrasonic signals need to be truncated to extract the wave features, and the rest of the information is discarded. A few hand-picked features are extracted from this reduced data. So, to overcome the data reduction limitation a novel method extracting the ultrasonic features automatically from the entire signal is demonstrated using a deep learning framework. In this, the recorded ultrasonic signals are passed through a convolutional neural network (CNN) to extract the features automatically. Furthermore, feature importance and an optimum number of feature selections are carried out using the XGBoost method. Finally, Long Short-term Memory (LSTM) model is developed using the time history of these features to predict the failure. Results show that the timing and size of the failure can be predicted with high confidence.

The data-driven models require training on large datasets and overlook the physical laws controlling the shear failure. As such, the model may perform well for a particular dataset but fail to provide satisfactory predictions for a different albeit closely related dataset. To incorporate the domain knowledge and address the model transferability challenge, in this study, a physics-informed deep learning approach is also implemented to forecast failure. The data-driven predictions obtained using the Multi-layer Perceptron (MLP) & LSTM model are used as a baseline. Along with shear stress, the shear failure rate (fault slip rate) is also predicted and used in the physical constraint formulations. The rate-and-state friction law and elastic coupling relation are integrated into the deep learning model architecture to modify the loss function. We hypothesize that a proposed physics-informed deep learning framework can improve model generalizability, prediction of an earthquake, and micro-seismicity informed by the physics laws dictating the shear failure state.

## Bottom-up Implementation of Hardware Security primitives on 2D Materials

*Aaryan Oberoi*

PI: Dr. Saptarshi Das

**Abstract:** The rapid proliferation of security compromised hardware in today's integrated circuit (IC) supply chain poses a global threat to the reliability of communication, computing, and control systems. Critical information pertaining to national security is often put at stake due to weak copyright protection measures, conspicuous techniques to camouflage chip functionality and guesstimated hardware-assisted threat-defense models. While there have been significant advancements in detection and avoidance of security breaches, current standards are still inadequate, inefficient, often inconclusive, and resource extensive in both time and cost, offering tremendous scope for innovation in this field. Here, we experimentally demonstrate a fully integrated hardware chip based on two-dimensional (2D) MoS<sub>2</sub> field-effect transistors (FETs), capable of detecting/avoiding authenticity threats like, cloning, reverse engineering, recycling, and remarking. We utilize the inherent variation, sensing and programmability aspects to show a full-scale implementation of different security primitives like physically unclonable function (PUF), hardware usage counter, intellectual property (IP) watermarking and camouflaging of integrated circuit (IC), covering material level to circuit level on a single chip. We exploit the material disorder over large area grown MoS<sub>2</sub> film for use as a PUF and show its reconfigurability aspects. We then offer a non-volatile memory based on MoS<sub>2</sub> FET for use as an electronic counter to meter the usages of the chip. We further utilize the optical sensing capability of the MoS<sub>2</sub> to uncover an authentication signature, concealed in an array of MoS<sub>2</sub> FETs. Furthermore, we camouflage the true functionality of a 2-bit digital-to-analog converter (DAC) and an NMOS inverter circuit by optically programming the resistance values of specific MoS<sub>2</sub> FETs in the circuit. Our bottom-up hardware security integration from material to circuit level on high performance MoS<sub>2</sub> FETs is the first demonstration of an all-in-one security-enabled chip protected with major security primitives.

## **Tension-Tension Fatigue Behavior of Carbon/Epoxy Composites with Concentrated Carbon Nanotube Interlayers for High Damping**

*Avery Brown*

Future goals for high-speed rotorcraft demand a rigid/hingeless rotor with the ability to passively dampen vibrations. Damping in lightweight carbon fiber reinforced epoxy (c/ep) composites, which are commonly used to manufacture rotorcraft blades, can be enhanced by adding carbon nanotubes (CNTs) to the material. The mechanism of damping is interfacial slippage between the CNTs and the matrix. A fundamental question about this lightweight approach for adding damping in c/ep composites is whether the addition of CNTs to c/ep laminates affects the durability of the material under the fatigue loading conditions experienced by rotorcraft blades. This investigation provides unique preliminary data on the tension-tension fatigue behavior of c/ep composites with CNTs concentrated in the interlayer regions between the c/ep layer. Two separate maximum cyclic strain levels, 3000 and 4000  $\mu\text{m/m}$ , were selected as strains representing the upper end of plausible strains in blades. The effect of CNT alignment was investigated by poorly-aligned CNT yarns and well-aligned CNT film, with the alignment direction along the loading direction for maximum damping. For CNT yarn, Triton X-100 surface treatment was applied to half of the specimens to investigate if alteration of the interfacial bond strength between CNT and epoxy matrix changes fatigue behavior. Dynamic properties (loss factor, loss modulus and storage modulus), were measured at specific cycle increments during fatigue cycling to indirectly monitor progressive damage. Additionally, at the conclusion of fatigue testing, damage was nondestructively evaluated using penetrant-enhanced X-ray radiography. The results show that the addition of both types of CNT interlayers accelerates the formation and growth of matrix damage, leading to reduced storage modulus. The loss modulus generally increased with fatigue damage accumulation, although the increase was not consistent across different cyclic strain amplitudes. X-ray radiography showed that the aligned CNT interlayers cause delamination and the randomly oriented CNT interlayers were susceptible to matrix cracking along the directions of the off-axis carbon fibers.

## **Dynamic Mechanical Behavior of Carbon Nanotube Yarns**

*William Henry Dyer*

Advisor: Dr. Charles Bakis

Composites, especially carbon fiber reinforced epoxy composites, are a popular choice for aerospace structures because of their light weight relative to strength and stiffness. One such application is carbon/epoxy rotorcraft blades. These blades are subject to much vibration, thus high damping is needed in composite blades for next generation rotorcraft with increased speed capability. Research has been conducted into embedding different condensed forms of carbon nanotubes (CNTs) into composites in order to achieve this damping. One of these forms are CNT yarns, which are long, continuous, string-like threads of carbon nanotubes. While some studies have been conducted on composites with embedded CNT yarns, less research exists on the damping and mechanical properties of CNT yarns alone.

This presentation focuses on the characterization of carbon nanotube yarn through mechanical testing and analysis in order to better understand their behavior in composite laminates. Dry, as-received yarns, and epoxy-saturated yarns are tested dynamically and in quasi-static tension to determine mechanical properties and to study the effect of an epoxy matrix on the yarn. CNT yarns are also tested axially in compression to study compressive behavior. From tension tests, dry yarns are found to have an elastic modulus higher than that of resin-saturated yarns, but with much higher variability between specimens. It is also theorized from observations of tensile tests that yarns have a strain hardening-like ratcheting mechanism that increases the modulus over successive load cycles. Furthermore, the elastic modulus and strain-to-failure of resin-saturated yarns are found to be relatively insensitive to the stiffness of different matrices. Compression test results show that yarns do not experience detectable failure up to 2.3% strain, and suggest that yarns have no compressive strength. From dynamic mechanical analysis, it is found that with continued cycling and increased strain, the storage modulus of resin-saturated yarns sharply increases, while damping decreases.

# Tracking atomic-scale defects involved in metal-oxide-semiconductor device stressing with simple near-zero-field magnetoresistance measurements

*Stephen Moxim advised by Dr. Patrick Lenahan*

Electron paramagnetic resonance (EPR) techniques are unrivaled in their ability to study paramagnetic point defects in semiconductors and insulators. EPR has been used for decades to study such defects in bulk materials and large area thin films [1–6]. More recently, EPR measurements through electrically detected magnetic resonance (EDMR) have been utilized to study atomic scale defects in micro- and nanoscale devices. EDMR is roughly  $10^7$  times more sensitive than conventionally detected EPR [7,8], and is also exclusively selective to defects in the active areas of semiconductor devices. EDMR has been widely utilized to study defect generation in MOSFETs due to radiation damage [9], hot-carrier stress [10], and time-dependent dielectric breakdown (TDDB) [11]. EDMR measurements require a sensitive electrical detection scheme, the ability to sweep a magnetic field across the sample, and a microwave photon source. Although both conventional EPR and EPR detected via EDMR are powerful analytical techniques, they are complex and require a fairly expensive experimental apparatus.

We demonstrate that a recently developed analytical technique, near-zero-field magnetoresistance (NZFMR), is useful in tracking atomic-scale phenomena involved in the high-field stressing damage of fully processed Si MOSFETs. We show that the technique is sensitive to both the  $P_{b0}$  and  $P_{b1}$  dangling bond centers and that the presence of both centers can be inferred through NZFMR via hyperfine interactions with the central  $^{29}\text{Si}$  atoms of the dangling bonds. The NZFMR results also provide evidence for the redistribution of mobile hydrogen atoms at the Si/SiO<sub>2</sub> interface. This work provides a proof-of-concept demonstration that NZFMR offers much of the analytical power of electrically detected magnetic resonance when applied to a technologically important problem.

## References:

- [1] Y. Y. Kim and P. M. Lenahan, *J. Appl. Phys.* 64, 3551 (1988).
- [2] J. T. Yount, P. M. Lenahan, and G. J. Dunn, *IEEE Trans. Nucl. Sci.* 39, 2211 (1992).
- [3] J. T. Krick, P. M. Lenahan, and G. J. Dunn, *Appl. Phys. Lett.* 59, 3437 (1991).
- [4] G. J. Gerardi, E. H. Poindexter, P. J. Caplan, and N. M. Johnson, *Appl. Phys. Lett.* 49, 348 (1986).
- [5] W. L. Warren and P. M. Lenahan, *Appl. Phys. Lett.* 49, 1296 (1986).
- [6] W. L. Warren, P. M. Lenahan, and S. E. Curry, *Phys. Rev. Lett.* 65, 207 (1990).
- [7] M. Stutzmann, M. S. Brandt, and M. W. Bayerl, *J. Non. Cryst. Solids* 269, 1 (2000).
- [8] D. Kaplan, I. Solomon, and N. F. Mott, *J. Phys., Lett.* 39, 51 (1978).
- [9] M. A. Jupina and P. M. Lenahan, *IEEE Trans. Nucl. Sci.* 36, 1800 (1989).
- [10] J. W. Gabrys, P. M. Lenahan, and W. Weber, *Microelectron. Eng.* 22, 273 (1993).
- [11] J. H. Stathis, *Appl. Phys. Lett.* 68, 1669 (1996).

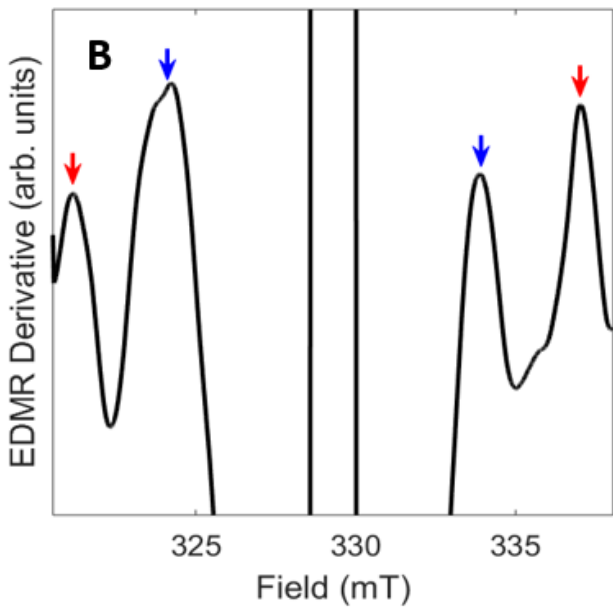
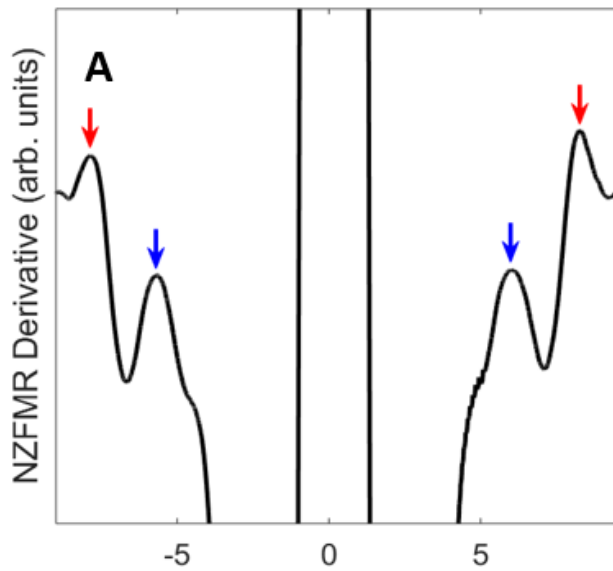


Fig. 1. NZFMR (top) and EDMR (bottom) results showing hyperfine features.

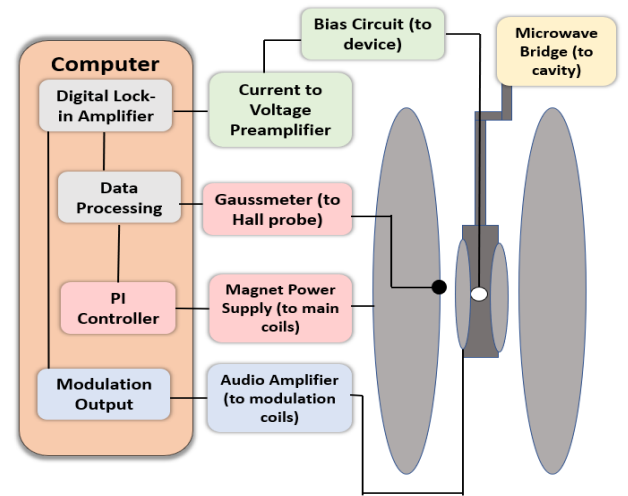
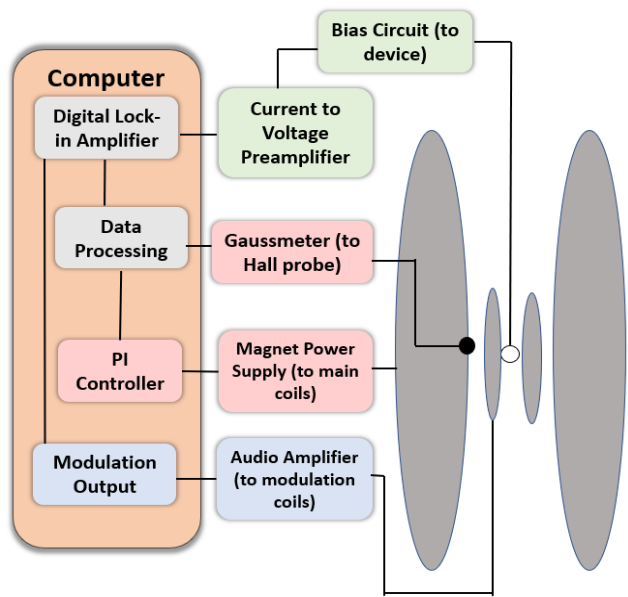


Fig. 2. NZFMR (top) and EDMR (bottom) spectrometer block diagrams.

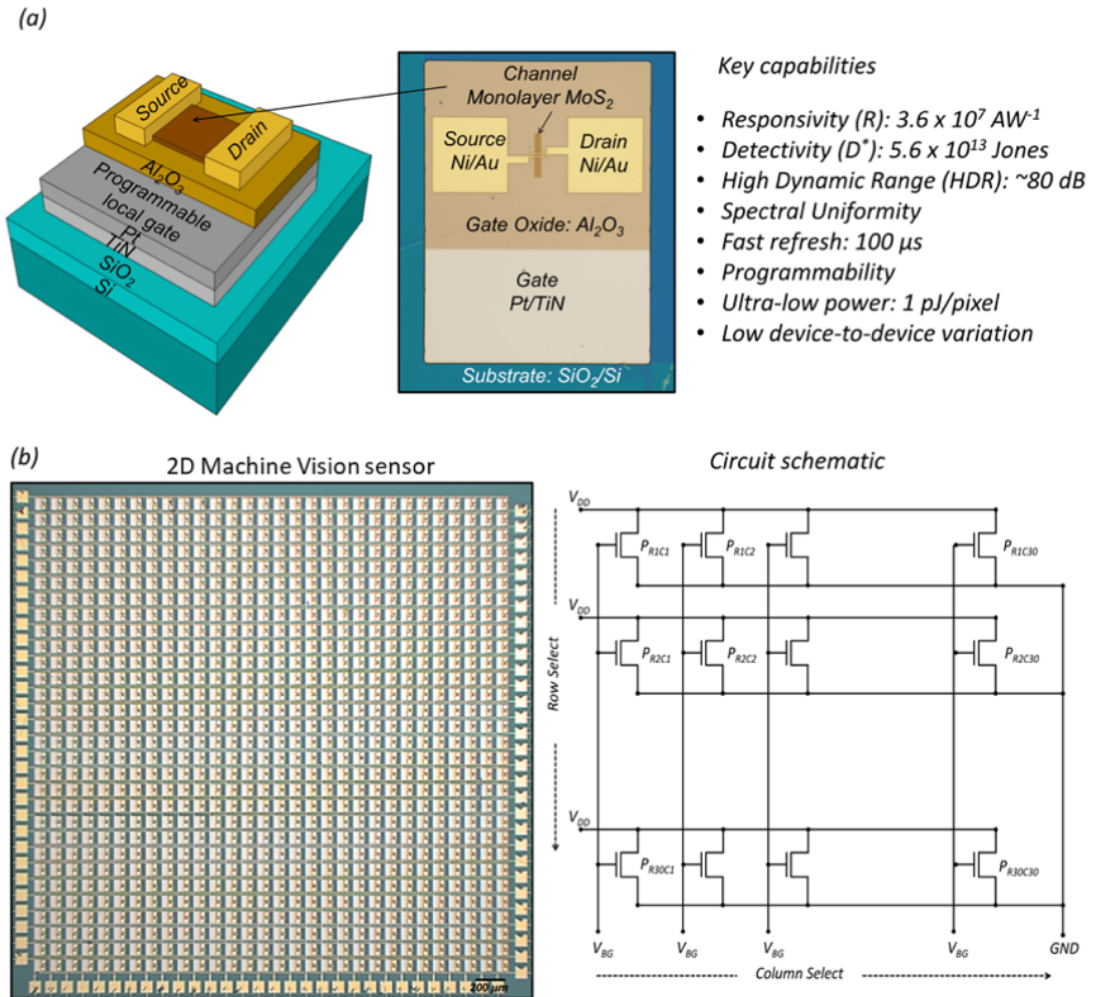
## **A Low-Power, Bio-inspired, Adaptive Machine Vision Sensor based on Atomically Thin Memtransistors**

*Akhil Dodda<sup>1</sup>, Darsith Jayachandran<sup>1</sup>, Andrew Pannone<sup>1</sup>, Yikai Zheng<sup>1</sup>, Abu Musa Abdullah<sup>1</sup>, Shiva Subbulakshmi Radhakrishnan<sup>1</sup>, Nichola Trainor<sup>2</sup>, Joan M Redwing<sup>1,2</sup> & Saptarshi Das<sup>1,2</sup>*

<sup>1</sup>Department of Engineering Science and Mechanics, Pennsylvania State University, University Park, PA 16802, USA

<sup>2</sup>Department of Material Science and Engineering, Pennsylvania State University, University Park, PA 16802, USA Email: aud430@psu.edu / Phone: (814)-206-4921

With the rapid advancements of information technology, the internet of things (IoT), and their integration; machine vision systems have become a crucial component in autonomous driving, robotics, security, autonomous production, and other domains. However, with the increase in the volume of data, new requirements are put-forward on the traditional hardware vision systems. In conventional machine vision systems, the optical information is projected onto the CMOS image sensors using a lensing system to convert the optical information into electrical currents which are further integrated using the read-out circuitry to generate voltage outputs. These generated voltage outputs are further converted into digital signals using analog to digital converter (ADC) and are communicated between the CPU and memory for information processing or pattern recognition. These image processing systems rely on von Neumann architectures and consume an enormous amount of energy while transmitting the data between processing and memory units, thereby, necessitating the need for material discovery, innovation in device design, and novel architectures to bridge the physical gap between the sensor, processor, and memory units. Acknowledging these limitations and deriving inspiration from the human visual system, we here propose and experimentally demonstrate a low-power, “all-in-one” hardware vision platform based on a monolayer MoS<sub>2</sub> phototransistor array integrated with a programmable gate-stack. We exploit the phenomenon of gate-tunable persistent photoconductivity or optical memory in MoS<sub>2</sub> phototransistors for in-sensor storage of visual information. Also, leveraging the merits of gate-tunable persistent photoconductivity we also demonstrate a record-high responsivity of  $\sim 3.6 \times 10^7$  A/W and a record-high detectivity of  $\sim 5.6 \times 10^{13}$  Jones. Furthermore, we demonstrate analog level learning to different illumination wavelengths and learning adaptation to different illumination levels and illumination wavelengths in the visible spectrum. In addition to persistent photoconductivity, we exploit the gate-voltage induced analog and non-volatile threshold voltage shift in MoS<sub>2</sub> phototransistors for gradual or immediate forgetting of the stored information. We demonstrate the dynamic learning and relearning of the input patterns from external visual stimuli by combining optical learning and electrical forgetting in our MoS<sub>2</sub> phototransistor. Finally, we show the efficacy of our learning and forgetting mechanism at noisy illumination conditions under high signal-to-noise ratios. Overall, the amount of energy consumed in performing the learning, relearning, and forgetting by our hardware vision platform was found to be a few tens of nano Joules highlighting the benefits of our hardware vision platform for designing next-generation machine intelligent systems.



a) 3D schematic, optical image, and key features of a 2D APS based on monolayer MoS<sub>2</sub> phototransistor integrated with a programmable gate stack comprising of 50 nm Al<sub>2</sub>O<sub>3</sub> on Pt/TiN patterned as islands on top of a Si/SiO<sub>2</sub> substrate. b) Optical image of a 900-pixel 2D APS fabricated in a crossbar architecture and the corresponding circuit diagram showing the row and column select lines.

## **Algorithm for Grain Size Analysis and Phase Segmentation (AGAPS)**

*Christopher Wheatley Jr, Dr. Andrea P. Argüelles*

Micrographs provide crucial data for material characterization because of the large variety of macroscopic properties that can be estimated from them, such as elastic moduli, mechanical behavior, and phase composition. Our group compares data derived from ultrasonic nondestructive evaluation with optical micrographs to patterns in material properties. We have developed an automatic program to measure the two-point spatial correlation factor (SCF), which measures the probability that two random points in a microstructure fall within the same grain. SCF is important in microstructures because it can be used to estimate porosity, grain sizes, and other features in the micrograph. By selecting random points throughout the image, an accurate statistical distribution based on the microstructure can be measured regardless of the scale or particle shape in a given image. Our program segments multiphase micrographs into the different images that can then be individually analyzed to identify each phase's unique grains. Previous image segmentation programs could only describe SCF for each phase, but this program further segments individual grains within each phase to give increased information about the granular microstructure for multiphase materials. Estimates of porosity and effective pore size are obtained from the SCF.

# A Sparse and Spike-timing based Adaptive Photo Encoder for Augmenting Machine Vision for Spiking Neural Networks

*Dipanjan Sen*

Abstract:

Machine vision continues to push the limits of artificial intelligence (AI) in our everyday life, from automating surgeries to driving autonomous vehicles in crowded streets. Augmenting machine vision with biomimetic and bio-inspired functionalities can, therefore, benefit the development of future AI and bridge the energy gap with natural intelligence. In this context, spiking neural network (SNN) has received much attention since it imitates information processing inside natural brains using electrical impulses or spikes. While in animals, specialized afferent neurons transform external stimuli into sparse spiking, state-of-the-art machine vision platform are inept in doing so and require extensive circuitry which add energy and area overhead. Here we design a medium scale integrated (MSI) circuit comprising of two three-stage ring oscillators (RO) and one XOR logic gate fabricated using a total of 21 memtransistors based on photosensitive two-dimensional (2D) monolayer MoS<sub>2</sub> for spike-timing based encoding of visual information. We show that different illumination intensities can be encoded into sparse spiking with time-to-first-spike representing the illumination information, i.e., higher intensities invoke earlier spikes and vice versa. In addition, non-volatile and analog programmability of our photo encoder is exploited for adaptive photo encoding that allows expedited spiking under scotopic (low light) and deferred spiking under photopic (bright light) conditions, respectively. Our design has a small footprint with an active device area of  $\sim 100 \mu\text{m}^2$  and consumes miniscule energy less than  $1 \mu\text{J}$  to accomplish the photo encoding functionality. Our demonstration of in-sensor photo encoder exploiting programmable optoelectronic circuits based on 2D memtransistors can be transformative for next generations of machine vision applications.

## **Application of Multidomain Image Data Fusion For Enhanced Convolutional Neural Network Classification**

*Ferris Arnous*

Convolutional neural networks (CNNs) provide the sensing and detection community with a discriminative approach for classifying images. However, one of the largest limitations for deep CNN image classifiers is the need for extensive training datasets containing a variety of image representations. While current methods such as GAN data augmentation, additions of noise, rotations, and translations can allow CNNs to better associate new images and their feature representations to ones of a learned image class, many fail to provide new contexts of ground truth feature information. To expand the association of critical class features within CNN image training datasets, an image pairing and training dataset augmentation paradigm via a multi-sensor domain image data fusion algorithm is proposed. This algorithm uses a mutual information and merit-based feature selection subroutine to pair highly correlated cross domain images from multiple sensor domain image datasets. It then re-augments the corresponding cross domain image pairs into the opposite sensor domain's feature set via a highest mutual information, cross sensor domain, image concatenation function. This augmented image set then acts to retrain the CNN to recognize greater generalizations of image class features via cross-domain, mixed representations. Our experimental results indicated an increased ability of CNNs to generalize and discriminate between image classes during testing of class images from SAR vehicle, solar cell device reliability screening and lung cancer detection image datasets.

# **A Monolithic Stochastic Computing Architecture for Energy Efficient Arithmetic Enabled by 2D Memtransistors**

*Harikrishnan Ravichandran*  
*Advisor: Dr. Saptarshi Das*

**Abstract:** As the computing algorithms become more complex and the amount of data to be processed increase, the energy and hardware investments necessary for conventional high-precision digital computing continues to explode in the emerging era of artificial intelligence, deep learning, and Big-data. This has necessitated an investigation into alternative forms of computing that require limited hardware and energy resources. Stochastic computing (SC) is an attractive alternative since it enables arithmetic operations such as addition, subtraction, multiplication, sorting, etc., using simple logic gates with minimal hardware and energy investment along with resilience to bit error [1]. SC relies on the generation of stochastic bits (s-bit) of desired probabilities to perform arithmetic operations. SC architecture based on traditional silicon complementary metal-oxide semiconductor (CMOS) [2] technology requires significant hardware investment to generate stochastic bits. Memristor [3] and spin-based devices [4] offer natural randomness but depend on hybrid designs involving CMOS peripherals for accelerating SC, which increases area and energy burden. Here we propose and experimentally demonstrate a standalone SC architecture embedded in memory based on two-dimensional (2D) memtransistors. We use only a six-transistor (6T cell) to realize an s-bit generator circuit that exploits the inherent stochasticity in the carrier trapping and detrapping phenomena in the gate insulator of the 2D memtransistors and combines it with an inverting amplifier and a programmable thresholding inverter to obtain s-bits. The s-bits are then integrated with 2D memtransistor based logic gates such as MUX, XOR, AND, OR, and NOT gates to demonstrate arithmetic operations such as addition, subtraction, multiplication, and sorting. Our monolithic and non-von Neumann SC architecture consumes a miniscule amount of energy  $< 1$  nano Joules for s-bit generation and to perform arithmetic operations highlighting the benefits of SC.

## **References:**

- [1] B. R. Gaines, "Stochastic computing," in Proceedings of the April 18-20, 1967, spring joint computer conference, 1967, pp. 149-156.
- [2] S. C. Smithson, N. Onizawa, B. H. Meyer, W. J. Gross, and T. Hanyu, "Efficient CMOS invertible logic using stochastic computing," IEEE Transactions on Circuits and Systems I: Regular Papers, vol. 66, pp. 2263-2274, 2019.
- [3] P. Knag, W. Lu, and Z. Zhang, "A native stochastic computing architecture enabled by memristors," IEEE Transactions on Nanotechnology, vol. 13, pp. 283-293, 2014.
- [4] R. Venkatesan, S. Venkataramani, X. Fong, K. Roy, and A. Raghunathan, "Spintastic: Spin-based stochastic logic for energy-efficient computing," in 2015 Design, Automation & Test in Europe Conference & Exhibition (DATE), 2015, pp. 1575-1578.

## **An All-in-One 2D Neuromorphic System**

*Shiva Subbulakshmi Radhakrishnan*

Artificial neural networks exist for very long time now, and they have almost pushed the boundaries since they need high power GPUs to perform their computation. Most of the ANN computations consist of vector matrix multiplication which requires frequent data-shuttle between memory and compute unit which makes it hard to realize in traditional electronic devices. In contrast human brain consumes only 20W of power despite doing all sorts of computations and decision making. Human brain performs in-memory compute whereas our traditional electronic devices perform Von-Neuman computing which makes it energy intensive for performing vector matrix multiplication. Here we exploit sensing, computing, and programmable memory devices based on emerging two-dimensional (2D) layered materials such as MoS<sub>2</sub> to demonstrate a monolithically integrated, multi-pixel, adaptive, and “all-in-one” hardware neuromorphic system capable of learning, forgetting, and inferring at miniscule energy expenditure. Our findings highlight the potential of multifunctional 2D materials in developing in-sensor and near-sensor compute and storage capabilities that can not only overcome the bottleneck of von Neumann architecture used by conventional silicon-based complementary metal oxide semiconductor (CMOS) technology but also eliminates the need for CMOS peripherals, which is unavoidable for competing non-von Neumann technologies such as memristors.

## Modeling Fungal Infections: Matrix Development in Zombie Ants

*F. Ghanbari\**, *F. Costanzo<sup>†</sup>*, *D. Hughes<sup>‡</sup>*, *C. Peco<sup>§</sup>*

\* Engineering Science and Mechanics, Penn State University, State College, USA  
Email: [farshad.ghanbari@psu.edu](mailto:farshad.ghanbari@psu.edu)

<sup>†</sup> Engineering Science and Mechanics, Penn State University, State College, USA  
Email: [fxc8@psu.edu](mailto:fxc8@psu.edu)

<sup>‡</sup> Department of Entomology, Penn State University, State College, USA  
Email: [dhughes@psu.edu](mailto:dhughes@psu.edu)

<sup>§</sup> Engineering Science and Mechanics, Penn State University, State College, USA  
Email: [christian.peco@psu.edu](mailto:christian.peco@psu.edu)

Modeling how infections spread within the body of insects and other animals is of critical interest to fields like medicine and biotechnology. Beyond the intrinsic interest to entomologists and biologists, there are some common features between disease spreading processes in the human body and insects [1]. The knowledge acquired from their study can be used to better understand the mechanical and chemical interactions governing an infectious mass, and to provide insights to efficiently inhibit its advance, once the key factors have been identified. In this poster, we present the first stage in the modeling of the spreading of the fungus *O. Unilateralis* within the head of its host, the ant *Camponotus Leonardi*, endemic to Brazil. We focus on the development of a model able to reproduce general features of fungal growth, such as the formation of exploratory networks. We propose mechanisms that are able to explain the muscle cell colonization process as it is observed in the infected ants, and then we illustrate the performance of our model with simulations that explore a wide range of initial conditions and parameters. We test our model against laboratory experiments to answer some fundamental questions in fungal infection within biological tissue.

### REFERENCES

[1] M. A. Fredericksen, Y. Zhang, M. L. Hazen, R. G. Loreto, C. A. Mangold, D. Z. Chen, and D. P. Hughes, “Three-dimensional visualization and a deep-learning model reveal complex fungal parasite networks in behaviorally manipulated ants,” *Proceedings of the National Academy of Sciences*, vol. 114, no. 47, pp. 12 590–12 595, 2017.

## miRNA Induced 3D Bioprinted-Heterotypic Osteochondral Interface

*Nazmiye Celik<sup>1,2</sup>, Myoung Hwan Kim<sup>2,3</sup>, Miji Yeo<sup>1,2</sup>, Fadia Kamal<sup>4</sup>, Daniel J. Hayes<sup>2,3,5,\*</sup>,  
Ibrahim T. Ozbolat<sup>1,2,3,5,6,\*\*</sup>*

<sup>1</sup>Department of Engineering Science and Mechanics, Penn State University, 212 Earth-Engineering Sciences Bldg., University Park, PA 16802, USA

<sup>2</sup>The Huck Institutes of the Life Sciences, Penn State University, University Park, PA 16802, USA.

<sup>3</sup>Department of Biomedical Engineering, Penn State University, Chemical and Biomedical Engineering Bldg., University Park, PA 16802, USA.

<sup>4</sup>Center for Orthopedic Research and Translational Sciences, Department of Orthopedics and Rehabilitation, Penn State University, Hershey, PA 17033, USA.

<sup>5</sup>Materials Research Institute, Penn State University, University Park, PA 16802, USA.

<sup>6</sup>Department of Neurosurgery, Penn State College of Medicine, Hershey, PA 17033, USA.

Engineering of osteochondral interfaces remains a challenge, particularly in providing suitable strategies for regeneration of lesions in cartilage and subchondral bone. MicroRNAs (miRs) have emerged as significant tools to regulate the differentiation and proliferation of osteogenic and chondrogenic formation in the human musculoskeletal system. Here, we describe a novel approach to osteochondral regeneration based on three-dimensional (3D) bioprinting of miR-transfected adipose-derived stem cell (ADSC) spheroids to produce a heterotypic interface that addresses the limited capacity of articular cartilage to self-repair itself and intrinsic limitations of the traditional approach in inducing zonal differentiation via the use of diffusible cytokines. We evaluated the delivery of miR-148b for osteogenic differentiation and the codelivery of miR-140 and miR-21 for chondrogenic differentiation of ADSC spheroids. Our results demonstrated that miR-transfected ADSC spheroids exhibited upregulated expression of osteogenic and chondrogenic differentiation related gene and protein markers, and enhanced mineralization and cell proliferation compared to spheroids differentiated using commercially-available differentiation medium. Upon confirmation of osteogenic and chondrogenic potential of miR-transfected ADSC spheroids, using aspiration-assisted bioprinting, these spheroids were 3D bioprinted into a dual-layer heterotypic osteochondral interface with stratified arrangement of distinct osteogenic and chondrogenic zones. The proposed approach holds great promise in biofabrication of stratified tissues, not only for osteochondral interfaces presented in this work, but also for other composite tissues and tissue interfaces, such as but not limited to bone-tendon-muscle interface and craniofacial tissues.

## **Spatial characterization approach for understanding Fabrication-Microstructure-Property relationships of Titanium rich LDED based Nitinol along overlap of passes and layers interfaces**

*Arnab Chatterjee<sup>1†</sup>, Reginald F. Hamilton<sup>1†</sup> \**

A criterion for optimal shape memory behavior is a crystallographic reversible phase transformation, commonly referred to as thermoelasticity. The underlying microstructural constituents like grain morphology, precipitate distribution and morphology, composition play an important role in controlling the local strain fields in the material which in turn controls the extent to which an SMA undergoes thermoelastic phase transformation. Thus, spatial characterization of these microstructural constituents is important. Conventional wrought Shape Memory Alloys (SMA) processing, however, aims to produce homogeneous properties and thus microstructures for promoting thermoelastic Martensitic Transformations (MTs). Additive Manufacturing (AM) is a layer-by-layer buildup technique for 3D printing/deposition of structures. The resulting microstructures are inherently heterogenous at multiple length scales like composition, structure, crystallographic phases, and microstructure. For this work, we fabricated Ti-rich compositions of NiTi SMAs using the Laser Directed Energy Deposition (LDED) AM technique. For LDED AM, pre-blended elemental Nickel and Titanium powder feedstock is injected through coaxial nozzles into a melt pool generated by a focused laser beam. The resulting microstructure can be designed by tuning build parameters such as the number of layers and passes, laser power, scanning velocity, hatch spacing, layer height, etc. We use multiscale characterization approaches for understanding the effect of LDED AM build parameter on microstructural hierarchy by spatially characterizing the heterogeneity in microstructural constituents generated along overlapping passes/layers interfaces and the effect of these structures/substructures on mechanical properties like microhardness. In this work, the number of layers and passes are varied and two build plans are manufactured one having 8 passes with 30 layers and other second having 4 passes with 58 layers. The plans are differentiated by the orientation of the tool path with respect to the mechanical loading direction. It has been observed that the FT (8 hatches x 30 layers) sample has larger variability of microstructural constituents, lower volume fraction of second phase, finer grains with low aspect ratio along with higher microhardness compared to the ST (4 hatches x 58 layers) specimen. A study of this variability would lead to understanding fabrication-microstructure-property relationships for Titanium-rich LDED based builds along overlapping interfaces.

## **Probing the micromechanical features of a fracture interface using a multi-physics approach: A numerical investigation relating asperity deformation with fluid flow**

*Clay Wood<sup>1</sup>, Chun-Yu Ke<sup>2</sup>, Andy Rathbun<sup>3</sup>, Jacques Rivière<sup>2</sup>, Derek Elsworth<sup>4, 1</sup>,  
Chris Marone<sup>1, 5</sup>, Parisa Shokouhi<sup>2</sup>*

<sup>1</sup>Dept. of Geosciences, Pennsylvania State University

<sup>2</sup>Dept. of Engineering Science and Mechanics, Pennsylvania State University

<sup>3</sup>Chevron ETC, San Ramon, CA, 94583, USA

<sup>4</sup>Dept. of Energy and Mineral Engineering, EMS Energy Institute, and G3 Center, Pennsylvania State University

<sup>5</sup>Dipartimento di Scienze della Terra, La Sapienza Università di Roma

The focus of this study is to elucidate the relation between elastodynamic and hydraulic properties of fractured rock subjected to local stress perturbations in relation to fracture aperture distribution. The goal of our integrated numerical and experimental investigations is to understand the mechanisms responsible for changes in fault zone permeability and elasticity in response to dynamic stressing in the subsurface (anthropogenic or seismic in origin). High-resolution (micron-scale) optical profilometry measurements combined with pressure sensitive films have been used to characterize fracture properties such as ‘true’ contact area, aperture distribution and morphology, as well as asperity deformation under applied loads in our experiments. These measurements allow a direct correlation between fracture properties and our lab measurements of fracture elastic nonlinearity and permeability. Using micron-resolution profilometry of centimeter-scale samples, we calculate the elastic deformation of fracture asperities to varying applied stresses (static and dynamic) using Hertzian contact mechanics. Then, permeability is calculated for each applied stress (deformed asperities) using the parallel plate approximation, in which the Reynolds equation is solved using the finite difference method. This study is uniquely constrained, wherein we investigate the effect of measured deformation of real asperities on creating flow pathways through a fracture. Future work will include implementing contact acoustic nonlinearity (CAN) to model the change in transmission of acoustic waves across the fracture interface during stress perturbation.

## Ultrasonic scattering from subwavelength cracks in anisotropic silicon

*L. Katch, and A. Argüelles*

**Abstract:** Silicon wafers, commonly used in the photovoltaic industry, are susceptible to cracking during manufacturing and processing that may impact their performance. These microscale cracks are difficult to detect ultrasonically due to the anisotropic nature of silicon and the high frequencies necessary for inspection. For instance, phased array (PA) approaches commonly used to detect and size cracks are unsuitable for this application due to the frequency constraints of commercial PA systems. Therefore, crack scattering in anisotropic media has mostly been studied from a theoretical perspective and little work has been done from an experimental lens. In this presentation, we experimentally evaluate ultrasonic scattering from cracks in submillimeter silicon wafers using single-element 100 MHz probes. We use an oblique-incidence, pulse-echo configuration to spatially map shear scattering from cracks at different orientations in orthotropic silicon samples. Our results illustrate the strong scattering dependence on crystal orientation and elucidate the complexities in the response as a function of the planes of symmetry. These results will enable more in-depth sensitivity analysis for crack detection and characterization in anisotropic samples.

## A Robust Insect Inspired Spike-based Collision Detector

*Mayukh Das, Dipanjan Sen, Darsith Jayachandran, Andrew Pannone, Saptarshi Das*

With increasing application of locomotive robots and autonomous vehicles in navigating unpredictable and often difficult terrains, evasion from both stationary and moving obstacles is a pertinent requirement. Meticulous and timely evaluation of potential impact/collision scenarios is necessary to provide ample opportunity for a route correction response or evasive maneuver. Contemporary state of the art technologies as LiDAR, Radar, ultrasonic sensors, and cameras suffers either from their own limitations in usage or are extremely uneconomical in terms of energy or require additional peripherals for functioning, regarding them unfit for working in resource constrained environments. However, several insects as flies, locusts can evade collision consuming very minimal energy owing to a specialized neuron called the Lobula Global Movement Detector (LGMD) that detects an impending collision and performs non-linear computations to chart an escape response. The looming stimulus from an approaching object from the photoreceptors in the insect eye is converted to an excitatory and an inhibitory response at the two dendritic branches of the LGMD neuron which results in non-monotonic firing of the LGMD neuron. This alerts the insect to generate an action potential to the motor neurons to change trajectory. Contemporary silicon-based complimentary metal-oxide semiconductor collision detectors based on insect-vision suffer from high area and energy consumption due to considerable physical distance between sensing and compute elements as well as the absence of sparse spike-based information processing. We present an insect-inspired reconfigurable optoelectronic Medium Scale Integrated Circuit consisting of three 2D MoS<sub>2</sub> based photosensitive memtransistors which use spike-based in-sensor computation to detect collision. It uses a combination of n-MOS transistors to generate the excitatory and inhibitory response on a looming light stimulus and performs an AND logic operation to generate the collision warning response. Our device has a very low energy footprint of only a few nano-Joules and a small area of 40  $\mu\text{m}^2$ .

## **Proton Conductivity in Squid Ting Teeth Protein Membrane**

*Adam Alavi*

Proton conductivity is a naturally occurring process that has growing potential in solid-state electrical and energy applications. Protein based materials have certain advantages when compared to ion-conductive materials for industrial-scale powering equipment. Features such as biocompatibility, tunable structures, self-healing ability, and control of material properties make squid ring teeth (SRT) proteins a viable candidate for biosensing and biodetecting devices.

Previous studies of bulk proton conductivity in tandem repeat protein sequences of SRT have been performed by Pena-Francesch et al. who showed that tandem repetition of sequences of SRT significantly and systematically increased bulk proton transport. Pena-Francesch et al. used a fabrication process that involved a buffer solution to create the proteins. This construction method from 2018 has since been upgraded to produce higher yields of protein by replacing the buffer solution step with a DMSO purification step. This change in the fabrication process warrants a retesting of the bulk proton conductivity of the newly created proteins to determine if the change in the production process had any effect on the material's ability to transport protons. The study will be pushed further as new aromatic amino acid sequences have been proposed to further enhance the bulk protonic transport properties.

## **Aspiration-assisted freeform bioprinting of mesenchymal stem cell spheroids within alginate microgels**

*Myoung Hwan Kim, Ibrahim Ozbolat*

Aspiration-assisted freeform bioprinting (AAfB) has emerged as a promising technique for precise placement of tissue spheroids in three-dimensional (3D) space enabling tissue fabrication. To achieve success in embedded bioprinting using AAfB, an ideal support bath should possess shear-thinning behavior and yield-stress to facilitate tight fusion and assembly of bioprinted spheroids forming tissues. Several studies have demonstrated support baths for embedded bioprinting in the past few years, yet a majority of these materials poses challenges due to their low biocompatibility, opaqueness, complex and prolonged preparation procedures, and limited spheroid fusion efficacy. In this study, to circumvent the aforementioned limitations, we present the feasibility of AAfB of human mesenchymal stem cell (hMSC) spheroids in alginate microgels as a support bath. Alginate microgels were first prepared with different particle sizes modulated by blending time and concentration, followed by determination of the optimal bioprinting conditions by the assessment of rheological properties, bioprintability, and spheroid fusion efficiency. The bioprinted and consequently self-assembled tissue structures made of hMSC spheroids were osteogenically induced for bone tissue formation. Alongside, we investigated the effects of peripheral blood monocyte-derived osteoclast incorporation into the hMSC spheroids in heterotypic bone tissue formation. We demonstrated that alginate microgels enabled unprecedented positional accuracy (~5%), transparency for visualization, and improved fusion efficiency (~97%) of bioprinted hMSC spheroids for bone fabrication. This study demonstrates the potential of using alginate microgels as a support bath for many different applications including but not limited to freeform bioprinting of spheroids, cell-laden hydrogels, and fugitive inks to form viable tissue constructs.

# Digital Translation Of Micrographs For Finite Element Modelling Of Mechanical Response.

*Michail Skiadopoulos*

Additive manufactured parts may contain microstructural defects such as microscopic pores and lack of fusion defects. The assessment of this microstructure is important as it affects the mechanical properties of the part. One of the most effective ways to evaluate microstructural properties is Ultrasonic Testing (UT) where the part is excited by a pulse and the characterization is done based on the analysis of the received distorted signal. It has been shown that characteristics like wave speed and attenuation can be associated with features like porosity, grain size etc. However, quantitative relations do not exist. We propose to use deep learning models to find relations between ultrasonic signals and the microstructural features. The input to such models is the UT signal but using deep learning, the feature extraction process is much more effective, leading to more accurate predictions of microstructural properties. One impediment to developing such data-drive models is the scarcity of labelled data, since because of the cost associated with actual experiments, the experimental datasets are limited to a few tens of signals. A significant improvement could be achieved, if the dataset for training, validation and testing was expanded with Finite Element (FE) simulation results. To create realistic FE models, the first step is to use information from available micrographs and to create model microstructures. Before performing dynamic wave propagation simulations, we need to ensure that the model accurately simulates the stress-strain relation. In this study, a detailed procedure is presented for the transformation of an optical micrograph to a CAD model, which is then used for quasi-static stress-strain simulation. The first part is accomplished using the in-built python image processing libraries.

The second part is completed using a Representational Volume Element Method (RVE) simulation in ABAQUS to obtain the material behaviour in terms of stress-strain relationship. It is shown that the simulated results match experimental results reported in the literature. The next steps include wave propagation simulation to simulate ultrasonic signals.

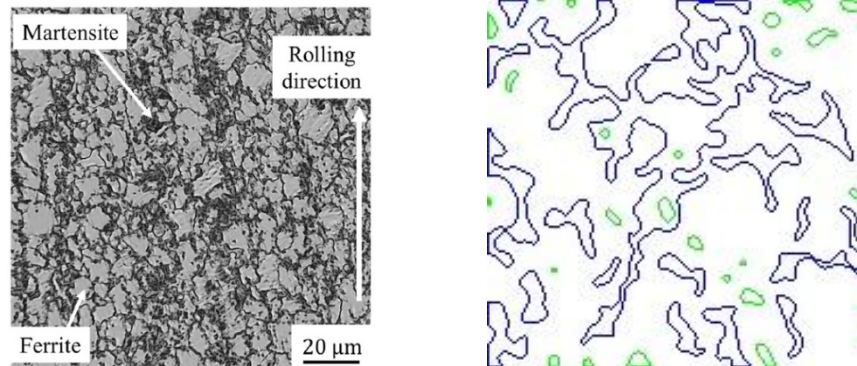


Fig 1. Image processing procedure. The grain contours are detect from the optical micrograph and the CAD model is created.

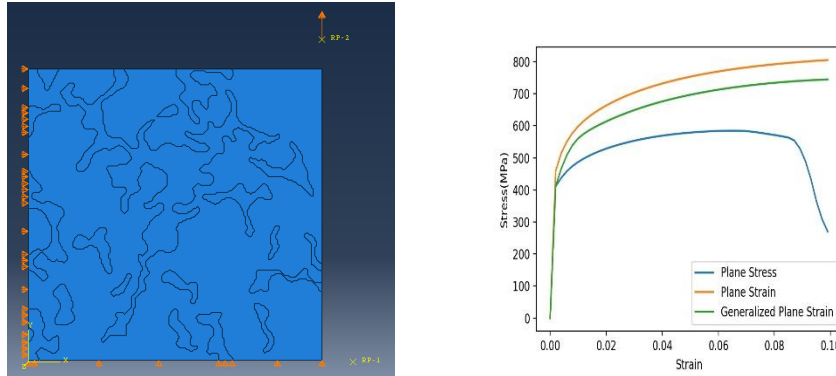


Fig 2. Plasticity simulation. The microstructure-informed CAD model is simulated with the RVE method and the material curve is obtained.

## References

- [1] *A random microstructure-based model to study the effect of the shape of reinforcement particles on the damage of elastoplastic particulate metal matrix composites*, Shaimaa I. Gad, Mohamed A. Attia, Mohamed A. Hassan, Ahmed G. El-Shafei Department of Mechanical Design and Production Engineering, Faculty of Engineering, Zagazig University, P.O. Box 44519, Zagazig, Egypt
- [2] *Micromechanics of multiaxial plasticity of DP600: Experiments and microstructural deformation modeling*, Shipin Qin, Ross McLendon, Victor Oancea , Allison M. Beese, Department of Materials Science and Engineering, Pennsylvania State University, University Park, PA 16802, United States, Dassault Systemes SIMULIA Corp., Johnston, RI 02919, United States
- [3] *Using Deep Image Collorization to Predict Microstructure-Dependent Strain Fields*, Pranav Milind Khanolkara , Aaron Abraham , Christopher McCombb , Saurabh Basua, Harold and Inge Marcus Department of Industrial Engineering, The Pennsylvania State University, State College 16802, US, School of Engineering Design, Technology and Professional Programs, The Pennsylvania State University, State College 16802, US
- [4] *Realistic microstructural RVEbased simulations of stress – strain behavior of a dual-phase steel having high martensite volume fraction*, J. Zhou, A.M. Gokhale, A. Gurusurthy, S.P. Bhat
- [5] *Influence of Mesoscale and Macroscale Heterogeneities in Metals on Higher Harmonics under Plastic Deformation*, Negar Kamali, Niloofar Tehrani, Amir Mostavi, Sheng-Wei Chi, Didem Ozevin, J. Ernesto Indacochea
- [6] *Characterization of heterogeneous microstructure in large forged products using nonlinear ultrasonic method*, Saju T. Abraham, S. Shivaprasad, C.R. Das, S. K. Albert, B. Venkatraman and Krishnan Balasubramaniam
- [7] *Microstructure-based model of nonlinear ultrasonic response in materials with distributed defects*, Saju T. Abraham, S. Shivaprasad, C.R. Das, S. K. Albert, B. Venkatraman and Krishnan Balasubramaniam

# Drawn-on-Skin Bioelectronics for Motion Artifact-Free Sensing and Point-of-Care Treatment

Faheem Ershad<sup>1</sup> and Cunjiang Yu<sup>1,2\*</sup>

<sup>1</sup>Department of Biomedical Engineering, Pennsylvania State University, State College, PA

<sup>2</sup>Department of Engineering Science and Mechanics, Pennsylvania State University, State College, PA

**Introduction:** Extraction of physiological and physical signals from human skin for health monitoring, disease prevention, and treatment is critical to sustain the wellbeing of humans. Recent advances in wearable bioelectronics which attach directly to the epidermal surface have suggested certain pathways. However, the existing wearable bioelectronics are susceptible to motion artifacts as they lack proper adhesion and conformal interfacing with the skin during motion. Here, we present ultra-conformal Drawn-on-Skin (DoS) electronics as a new bioelectronics platform for on-demand multifunctional, motion artifact-free sensing. DoS bioelectronics is created by liquid functional inks drawn into stencils using ballpoint pens directly on human skin. Upon drawing, an ultra-conformal, robust, and stretchable interface that is immune to motion is formed between DoS electronics and skin. This platform resolves the long-standing challenge of motion artifacts, without the need for additional hardware or computation.

**Materials and Methods:** The DoS devices are based on the Ag flakes/poly(3,4-ethylenedioxythiophene)-poly(styrenesulfonate) (Ag-PEDOT:PSS) composite, poly(3-hexylthiophene-2,5-diyl) nanofibrils (P3HT-NF), and ion gel as the conductive, semiconducting, and dielectric inks, respectively. The ink drawing characteristics, mechanical properties, skin compatibility, and electrical performances of the inks were evaluated. Devices such as transistors, heaters, strain, temperature, hydration, and electrophysiological (EP) sensors were developed (**Fig. 1a**) and characterized. The DoS EP sensors were compared to gel and mesh electrodes for their performance under motion during EP sensing. DoS electronics based electrical stimulation using a mouse model was performed to show accelerated wound healing.

**Results and Discussion:** The DoS inks can be easily drawn with sufficient resolution (~300  $\mu\text{m}$  line width), are mechanically stretchable up to 30%, do not cause any inflammatory response for up to 48 hrs according to histological studies, and have good electrical characteristics (conductive ink: 1.2  $\Omega/\text{sq}$ ) even under mechanical deformation. The signal-to-noise (SNR) ratios of the ECG signal perturbed by skin deformation (**Fig. 1b**) were 50, 20, and 12 dB for the DoS EP, gel, and mesh electrodes, respectively. Furthermore, the spectrogram showed that electromyogram (EMG) signal (<250 Hz) was not contaminated (**Fig. 1c**) by skin vibration when using the DoS EP sensors, unlike the others. In the wound healing experiment, electrical stimulation applied through custom DoS electrodes closed a skin wound about twice as fast as the control.

**Conclusion:** The inks, pens, and stencils serve as a toolkit for easy construction of customizable DoS devices and sensors, which are robust against motion artifacts. With further optimization of functional ink materials, sensor/device constructions and performances, studies of the sensor/device variability, and implementation of additional functionalities, DoS electronics can be implemented as a new, simple, and easily accessible yet promising personalized bioelectronics and healthcare tool.

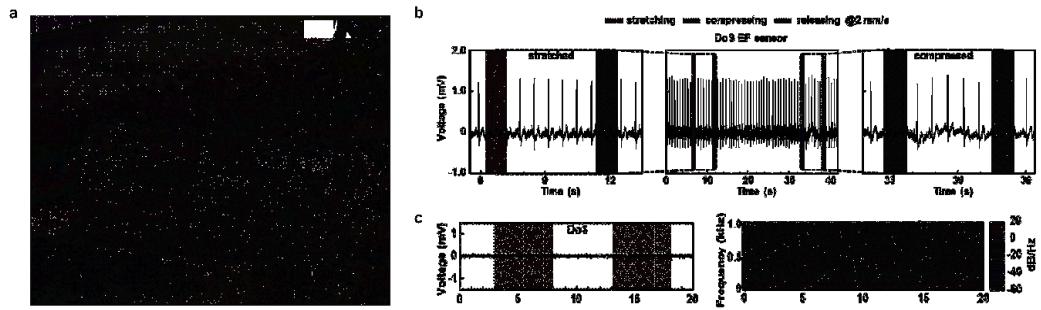


**Figure 1.** DoS electronics. a) Various DoS devices and sensors that can be fabricated on skin. b) ECG signals show no change in the waveform during various deformations. c) Vibrating the skin (pink sections) does not affect the EMG potentials in the time and time-frequency domains.

## **Contact and Non-Contact Characterization of Additively Manufactured and Wrought Samples**

*Evan Bozek*

Nonlinear resonance ultrasonic spectroscopy (NRUS) is a growing NDT technique for material characterization that is especially sensitive to small-scale defects such as microcracks. Previous studies using NRUS on Ti6Al4V additively manufactured (AM) samples show correlation between hysteretic nonlinearity ( $\alpha$ ) and the fatigue of a small population of samples, so it is of interest to use NRUS to evaluate the built quality of AM parts.

Most NRUS tests use a piezoelectric disc (PZT) bonded to the sample as an excitation source. Unfortunately, the bonding of the sample and the piezoelectric disc introduces additional nonlinearity, making it difficult to compare nonlinearity measured in different studies; error is also introduced by the gluing process, making repeated measurements less accurate. We evaluate the use of an air-coupled transducer as a non-contact excitation source for NRUS testing. We compare linear and nonlinear resonance measurements using contact and non-contact excitations on wrought and AM 316 stainless steel samples. We also look for trends between the different heat treatments and the NRUS measurements to see how microstructural changes from the heat treatments affect the measured ultrasonic properties.

Preliminary results show a significant reduction in the standard deviations of our linear measurements. The in-contact linear measurements show significant variation with repeated tests, while the non-contact linear measurements show nearly no variation, showing the potential for high accuracy measurements using air-coupled transducer excitation. The non-contact setup was unable to detect any nonlinearity in the samples, despite reaching the necessary strain level to exhibit nonlinearity.

### **3D Printed Microfluidics**

*Mecit Altan Alioglu*

Over the last decades, microfluidic devices have emerged rapidly as revolutionary, novel platforms for research and medicine. This was largely possible due to the invention of soft lithography. However, soft lithography is intrinsically expensive, time-consuming, and only convenient for fabricating 2D microfluidic channels. To overcome these challenges, researchers used 3D printing methods like Stereolithography (SLA), Fused Deposition Modeling (FDM), Multijet Modelling (MJM), Two-photon-polymerization (2PP). However, most of these existing strategies face considerable challenges in recreating delicate and intricate tissue-specific structural organizations. Herein, we present an alternative technique to fabricate complex 3D microfluidic channels with embedded 3D bioprinting. For embedded printing, a silicone elastomer gel mixture is cast into a mold as a support bath. Then, a sacrificial ink is printed inside the support bath using extrusion-based printing. After crosslinking the silicone elastomer support bath at high temperatures, the sacrificial ink is removed to obtain hollow microfluidic channels with resulting complex 3D geometries. This method allows for facile, rapid, scalable, cost-effective, and high-resolution printing and presents the potential to generate new insights for the developing microfluidic devices and bioprinting of large, vascularized tissue and organ models with biological functions.

## **Bioinspired Molecular Composites of 2D-Layered Materials and Tandem Repeat Proteins**

*Oguzhan Colak*

Protein materials endow biological systems with amazing capabilities, including tunable control of structural, optical, electrical, self-healing and thermal properties. Similarly, individual two-dimensional (2D) nanosheets show extraordinary mechanical, electronic, optical, and thermal properties. However, the brittle nature of 2D nanosheets drastically restricts manufacturing of flexible and stretchable composites. Inspired by natural composites, we designed stretchable materials with a critical structural length scale that are insensitive to flaws (e.g., for nacre at 1  $\mu\text{m}$ , bone at 100nm, whereas our approach around 2 nm). Here, we developed molecular-scale control of inter-layer spacing of 2D nanosheets by self-assembly of genetically engineered polymeric proteins to achieve mechanically compliant and ultra-tough composites. These engineered proteins adhere to 2D crystals via secondary structures (i.e., beta-sheets and alpha-helices), which are essential to maintain high strength and stretchability (i.e., toughness values of 52.6 MJ/m<sup>3</sup> and 58.5% fracture strain simultaneously). This mechanical deformation is over a factor of three larger than the current state-of-the-art stretchability for 2D composites, offering the possibility of engineering materials with reconfigurable physical properties.

## **A Comparative Study of Directed Energy Deposition (DED) and Powder Bed Fusion (PBF) Parts Using 316L Stainless Steel Powders**

*Raghul Asok Kumar*

Additive manufacturing has become a promising technology for the production of complex-shaped parts that are previously not possible. Directed Energy Deposition (DED) and Powder Bed Fusion (PBF) are the two widely used techniques to manufacture metal parts. In DED process, powders are fed simultaneously into the system while the laser melts them locally. With the PBF process, powders are spread and laser melting occurs layer by layer. DED process requires coarse powders for enhanced flowability through the nozzle while PBF process requires fine powders to be spread evenly before the laser melts them. A comparative study between the PBF and DED processes has been undertaken using gas atomized austenitic 316L stainless steel powders. Parts were manufactured through DED and PBF processes and were analyzed for their mechanical properties. The results show that parts produced by PBF process have superior tensile properties (YS  $588 \pm 4$  MPa, UTS  $722 \pm 5$  MPa, Elongation 55.5%) as compared to those produced by DED process (YS  $503 \pm 40$  MPa, UTS  $749 \pm 28$  MPa, Elongation 47.7%). The DED parts had higher hardness ( $229 \pm 12$  HV) as compared to the PBF parts ( $222 \pm 5$  HV). The effect of post processing of the parts like hot isostatic pressing (HIP) is also studied. Post HIP, DED parts seemed to improve their tensile properties while their hardness reduces as compared to PBF parts.

## Stacking Fault (SF) Mapping by 4DSTEM

*Yongwen Sun*

Nano-twins and stacking faults (SFs) are common planar defects in face-centered cubic (FCC) and hexagonal close-packed (HCP) metals. The existence of these two defects disrupts perfect symmetry in materials, so mechanical and electronic properties can be impacted favorably or unfavorably. Simultaneously, the interaction of these two defects can cause phase changing or mechanical property transformation. Therefore, quantitative SF classification and simultaneous mapping of SFs and TBs in an expanding field of view will bring convenience to the study of SF and nano-twin interaction and their effects on material performance. While Transmission Electron Microscopy (TEM) is a powerful characterization tool for detecting nanoscale interfacial structure, simultaneous mapping of SFs and nano-twins within a large field of view remains challenging. Here, by combining 4D-STEM and advanced data processing, two methods—virtual dark-field imaging and Bragg-peak distortion detection measurement, have been developed to address the issue of mapping SF at the scale of medium range. We further implemented these two methods to study defects in H-Nb<sub>2</sub>O<sub>5</sub>, a promising n-type semiconductor with a high dielectric constant utilized in solid electrolytic capacitors. Both methods can provide the nanometer resolution mapping of SFs, but the Bragg-peak distortion detection method offers a much better signal-to-noise ratio. Our methods offer quantitative SFs measurement with an expanding field of view, which will facilitate studies on the effects of SFs and nano-twins on the mechanical, electrical, and optical properties of engineering materials.

## **In-Memory Gaussian Synapses based on 2D CMOS FETs**

*Andrew Pannone*

Statistical analysis of univariate or multivariate data with an unknown probability distribution is a classical problem that necessitates probability density function estimation. Historically, parametric probability distributions have been used to analyze natural processes and predict the likelihood of outcomes in broad application scenarios such as risk estimation, healthcare, and product testing. Nonetheless, parametric density estimation methods often require supervised user input in the form of density function selection. Furthermore, these methods may struggle to accurately represent data that is either sparsely reported or distributed in an abnormal fashion. These limitations preclude parametric density estimation from application scenarios wherein data must be fit and analyzed at high frequencies without supervision such as traffic avoidance or ecological tracking. Non-parametric density function estimation via the Parzen window, commonly known as kernel density estimation (KDE) employs an algorithm that requires little to no supervision, can be adapted to any probability density, and is capable of converging on a target probability density with sparsely provided data.

Here, we have demonstrated monolithic heterogenous integration of complementary p-type Vanadium doped WSe<sub>2</sub> and monolayer n-type MoS<sub>2</sub> memtransistors to create 2T gaussian synapses that are used as kernels in the KDE algorithm. Each gaussian synapse is created by connecting the drain of an n-type MoS<sub>2</sub> memtransistor to the source of a p-type WSe<sub>2</sub> memtransistor as seen in figure 1. These memtransistors are biased in the subthreshold regime and consequently consume miniscule amounts of power. Based on the programmable and non-volatile memory state of each memtransistor, the mean, standard deviation, and amplitude of the resultant gaussian output characteristics can be manipulated and read at the common terminal. Figure 2 demonstrates the reconfigurable nature of the gaussian output characteristics. A population of gaussian synapses were fabricated and connected within a crossbar array where inputs are fed into the horizontal wordline and multiplication occurs at each node. Nodal output currents are then summed along the vertical bitline and read as a current output. This architecture collocates memory and computation by storing kernels as programmed gaussian synapses before performing summation of gaussian kernels to construct a probability distribution.

# Poster Presentations

Judges		Student Presenters							
		Aaryan Oberoi	Abhirup Saha	Arnab Chatterjee	Clay Wood	Faheem Ershad	Nazmiye Celik	Rahul Pendurthi	Yikai Zheng
Faculty	H. Tsosie	Judge			Judge		Judge		
	S. Das		Judge		Judge		Judge		
	A. Lakhtakia			Judge		Judge			Judge
	C. Peco		Judge	Judge			Judge		
	A. Arguelles	Judge		Judge				Judge	
	E. Sikora		Judge					Judge	Judge
	P. Shokouhi	Judge				Judge			Judge
	R. W. Smith		Judge		Judge		Judge		
	A. Geronimo				Judge	Judge		Judge	
Student	T. Sherry	Judge							
	Z. Rao		Judge			Judge			
	P. Manogharan			Judge				Judge	
	L. Katch	Judge			Judge				
	X. Li		Judge			Judge			
	D. Sen			Judge			Judge		
	D. Giraldo				Judge			Judge	
	R. Asokkumar					Judge			Judge
	I. Derman	Judge					Judge		
	V. Pal							Judge	Judge
	H. Ravichandran			Judge					Judge

## Bottom-up Implementation of Hardware Security primitives on 2D Materials

*Aaryan Oberoi*

PI: Dr. Saptarshi Das

**Abstract:** The rapid proliferation of security compromised hardware in today's integrated circuit (IC) supply chain poses a global threat to the reliability of communication, computing, and control systems. Critical information pertaining to national security is often put at stake due to weak copyright protection measures, conspicuous techniques to camouflage chip functionality and guesstimated hardware-assisted threat-defense models. While there have been significant advancements in detection and avoidance of security breaches, current standards are still inadequate, inefficient, often inconclusive, and resource extensive in both time and cost, offering tremendous scope for innovation in this field. Here, we experimentally demonstrate a fully integrated hardware chip based on two-dimensional (2D) MoS<sub>2</sub> field-effect transistors (FETs), capable of detecting/avoiding authenticity threats like, cloning, reverse engineering, recycling, and remarking. We utilize the inherent variation, sensing and programmability aspects to show a full-scale implementation of different security primitives like physically unclonable function (PUF), hardware usage counter, intellectual property (IP) watermarking and camouflaging of integrated circuit (IC), covering material level to circuit level on a single chip. We exploit the material disorder over large area grown MoS<sub>2</sub> film for use as a PUF and show its reconfigurability aspects. We then offer a non-volatile memory based on MoS<sub>2</sub> FET for use as an electronic counter to meter the usages of the chip. We further utilize the optical sensing capability of the MoS<sub>2</sub> to uncover an authentication signature, concealed in an array of MoS<sub>2</sub> FETs. Furthermore, we camouflage the true functionality of a 2-bit digital-to-analog converter (DAC) and an NMOS inverter circuit by optically programming the resistance values of specific MoS<sub>2</sub> FETs in the circuit. Our bottom-up hardware security integration from material to circuit level on high performance MoS<sub>2</sub> FETs is the first demonstration of an all-in-one security-enabled chip protected with major security primitives.

# **A Machine Learning Attack Resilient True Random Number Generator based on Stochastic Programmability in Two-Dimensional Transistors**

*By: Akshay Wali*

## **Abstract:**

Information exchange forms the heart of modern-day communications technology such as the Internet of Things (IoTs) that requires transmission of humongous volumes of data over increasingly complex networks. To guarantee security of encryption and decryption schemes for exchanging sensitive information, high quality random numbers are required. A true random number generator (TRNG) is a critical hardware component that guarantees such protection. Random numbers are widely used for information security, cryptography, stochastic modelling and banking and financing. In this article, we demonstrate a machine learning resilient TRNG by exploiting stochastic nature of carrier trapping and de-trapping phenomenon in a two-dimensional (2D) transistor with layered transition metal dichalcogenides (TMDs) such as tungsten diselenide ( $\text{WSe}_2$ ) and tungsten disulfide ( $\text{WS}_2$ ) as the channel material and a programmable gate stack consisting of a 50 nm alumina ( $\text{Al}_2\text{O}_3$ ) as the gate dielectric and a Pt/TiN/ $\text{p}^{++}$ -Si as the gate electrode. Our TRNG offers advantages in terms of circuit complexity and size since the randomness is derived from a single device. Furthermore, the generated bits pass the specified NIST Sp 800-22 rev. 1a randomness tests without any post-processing highlighting the potential of 2D-based hardware security primitives.

## **Spatial characterization approach for understanding Fabrication-Microstructure-Property relationships of Titanium rich LDED based Nitinol along overlap of passes and layers interfaces**

*Arnab Chatterjee<sup>1†</sup>, Reginald F. Hamilton<sup>1†</sup> \**

A criterion for optimal shape memory behavior is a crystallographic reversible phase transformation, commonly referred to as thermoelasticity. The underlying microstructural constituents like grain morphology, precipitate distribution and morphology, composition play an important role in controlling the local strain fields in the material which in turn controls the extent to which an SMA undergoes thermoelastic phase transformation. Thus, spatial characterization of these microstructural constituents is important. Conventional wrought Shape Memory Alloys (SMA) processing, however, aims to produce homogeneous properties and thus microstructures for promoting thermoelastic Martensitic Transformations (MTs). Additive Manufacturing (AM) is a layer-by-layer buildup technique for 3D printing/deposition of structures. The resulting microstructures are inherently heterogenous at multiple length scales like composition, structure, crystallographic phases, and microstructure. For this work, we fabricated Ti-rich compositions of NiTi SMAs using the Laser Directed Energy Deposition (LDED) AM technique. For LDED AM, pre-blended elemental Nickel and Titanium powder feedstock is injected through coaxial nozzles into a melt pool generated by a focused laser beam. The resulting microstructure can be designed by tuning build parameters such as the number of layers and passes, laser power, scanning velocity, hatch spacing, layer height, etc. We use multiscale characterization approaches for understanding the effect of LDED AM build parameter on microstructural hierarchy by spatially characterizing the heterogeneity in microstructural constituents generated along overlapping passes/layers interfaces and the effect of these structures/substructures on mechanical properties like microhardness. In this work, the number of layers and passes are varied and two build plans are manufactured one having 8 passes with 30 layers and other second having 4 passes with 58 layers. The plans are differentiated by the orientation of the tool path with respect to the mechanical loading direction. It has been observed that the FT (8 hatches x 30 layers) sample has larger variability of microstructural constituents, lower volume fraction of second phase, finer grains with low aspect ratio along with higher microhardness compared to the ST (4 hatches x 58 layers) specimen. A study of this variability would lead to understanding fabrication-microstructure-property relationships for Titanium-rich LDED based builds along overlapping interfaces.

## **Relating fracture aperture to hydro-mechanical properties of dynamically stressed tensile fractured rock**

*Clay Wood<sup>1</sup>, Prabhakaran Manogharan<sup>2</sup>, Jacques Rivière<sup>2</sup>, Derek Elsworth<sup>3, 1</sup>, Chris Marone<sup>1, 4</sup>, Parisa Shokouhi<sup>2</sup>*

<sup>1</sup>Dept. of Geosciences, Pennsylvania State University

<sup>2</sup>Dept. of Engineering Science and Mechanics, Pennsylvania State University

<sup>3</sup>Dept. of Energy and Mineral Engineering, EMS Energy Institute, and G3 Center, Pennsylvania State University

<sup>4</sup>Dipartimento di Scienze della Terra, La Sapienza Università di Roma

### **Poster Presentation**

The focus of this study is to elucidate the relation between elastodynamic and hydraulic properties of fractured media subjected to local stress perturbations in relation to fracture aperture distribution. Unique and well-controlled experiments are conducted on pre-fractured samples of Westerly granite under true-triaxial stress conditions and concurrent fluid flow of deionized water along the fracture. Pore pressure is oscillated at amplitudes ranging from 0.2 to 1 MPa at 1Hz to dynamically perturb the fracture. The experiments consider the influence of fracture aperture with perturbations at applied normal stresses 5 to 20 MPa (reducing aperture with increasing effective normal stress). During the dynamic stressing an array of piezoelectric transducers (PZTs) continuously transmit and receive ultrasonic pulses across the fracture to monitor the evolution of the elastic and hydraulic responses. Concurrent measurements of changes in ultrasonic wave velocity and amplitude driven by dynamic stressing are conducted to simultaneously measure the contact acoustic nonlinearity and permeability evolution. The evolution of fracture roughness and aperture with stress are imaged using two complementary techniques: (1) high resolution profilometry of fine-scale features and (2) mapping of impressions on pressure sensitive film at average stresses ranging from 3 to 21 MPa to monitor asperity deformation. The real area of contact and asperity deformation data from these imaging methods allow us to evaluate the openness/closedness across the surface. We compare ultrasonic velocity and RMS amplitude in regions predominately open to closed and then relate these results to the permeability to better understand clogging/unclogging mechanisms prevalent in pore fluid pressure oscillations. Future work includes laboratory experiments with fractures of different roughness and varying amounts of synthetic wear material and in developing a physics-based numerical simulation of laboratory experiments (accommodating high-resolution profilometry and experimental boundary conditions) to probe the micromechanical features of fractured rock interfaces.

## miRNA Induced 3D Bioprinted-Heterotypic Osteochondral Interface

*Nazmiye Celik<sup>1,2</sup>, Myoung Hwan Kim<sup>2,3</sup>, Miji Yeo<sup>1,2</sup>, Fadia Kamal<sup>4</sup>, Daniel J. Hayes<sup>2,3,5</sup>\*,  
Ibrahim T. Ozbolat<sup>1,2,3,5,6</sup>,\*\**

<sup>1</sup>Department of Engineering Science and Mechanics, Penn State University, 212 Earth-Engineering Sciences Bldg., University Park, PA 16802, USA

<sup>2</sup>The Huck Institutes of the Life Sciences, Penn State University, University Park, PA 16802, USA.

<sup>3</sup>Department of Biomedical Engineering, Penn State University, Chemical and Biomedical Engineering Bldg., University Park, PA 16802, USA.

<sup>4</sup>Center for Orthopedic Research and Translational Sciences, Department of Orthopedics and Rehabilitation, Penn State University, Hershey, PA 17033, USA.

<sup>5</sup>Materials Research Institute, Penn State University, University Park, PA 16802, USA.

<sup>6</sup>Department of Neurosurgery, Penn State College of Medicine, Hershey, PA 17033, USA.

Engineering of osteochondral interfaces remains a challenge, particularly in providing suitable strategies for regeneration of lesions in cartilage and subchondral bone. MicroRNAs (miRs) have emerged as significant tools to regulate the differentiation and proliferation of osteogenic and chondrogenic formation in the human musculoskeletal system. Here, we describe a novel approach to osteochondral regeneration based on three-dimensional (3D) bioprinting of miR-transfected adipose-derived stem cell (ADSC) spheroids to produce a heterotypic interface that addresses the limited capacity of articular cartilage to self-repair itself and intrinsic limitations of the traditional approach in inducing zonal differentiation via the use of diffusible cytokines. We evaluated the delivery of miR-148b for osteogenic differentiation and the codelivery of miR-140 and miR-21 for chondrogenic differentiation of ADSC spheroids. Our results demonstrated that miR-transfected ADSC spheroids exhibited upregulated expression of osteogenic and chondrogenic differentiation related gene and protein markers, and enhanced mineralization and cell proliferation compared to spheroids differentiated using commercially-available differentiation medium. Upon confirmation of osteogenic and chondrogenic potential of miR-transfected ADSC spheroids, using aspiration-assisted bioprinting, these spheroids were 3D bioprinted into a dual-layer heterotypic osteochondral interface with stratified arrangement of distinct osteogenic and chondrogenic zones. The proposed approach holds great promise in biofabrication of stratified tissues, not only for osteochondral interfaces presented in this work, but also for other composite tissues and tissue interfaces, such as but not limited to bone-tendon-muscle interface and craniofacial tissues.

## **Monolithic and Heterogeneous Integration of Atomically Thin Transition Metal Dichalcogenides for non von Neumann CMOS**

*Rahul Pendurthi<sup>1</sup>, Darsith Jayachandran<sup>1</sup>, Azimkhan Kozhakhmetov,<sup>2</sup> Nicholas Trainor<sup>2,3</sup>,  
Joshua A Robinson,<sup>2,3</sup> Joan M Redwing<sup>2,3</sup>, and Saptarshi Das<sup>2,3,4,\*</sup>*

*<sup>1</sup>Engineering Science and Mechanics, Penn State University, University Park, PA 16802, USA*

*<sup>2</sup>Materials Science and Engineering, Penn State University, University Park, PA 16802, USA*

*<sup>3</sup>Materials Research Institute, Penn State University, University Park, PA 16802, USA*

*<sup>4</sup>Electrical Engineering and Computer Science, Penn State University, University Park, PA 16802, USA*

Atomically thin, two-dimensional (2D), and semiconducting transition metal dichalcogenides (TMDs) are exciting candidates for replacing silicon based complementary metal oxide semiconductor (CMOS) technology in future nodes. While recent developments have shown high performance field effect transistors (FETs), logic gates, and integrated circuits (ICs) made from n-type TMDs, such as MoS<sub>2</sub> and WS<sub>2</sub> grown at wafer scale, realizing CMOS electronics necessitate monolithic integration of large area grown p-type semiconductors. Furthermore, the physical separation of memory and logic, which is used in von Neumann architecture, is a bottleneck of the existing CMOS technology to minimize energy consumption and maximize computational capabilities. Here, for the first time, monolithic and heterogeneous integration of large area grown n-type MoS<sub>2</sub> and p-type vanadium doped WSe<sub>2</sub> FETs with non-volatile and analog memory storage capabilities to achieve a non von Neumann 2D CMOS platform is demonstrated. The proposed manufacturing process flow allows for precise positioning of n-type and p-type FETs, which is critical for any IC development. Digital computing primitives, such as inverters and multiplexers, and neuromorphic computing primitives such as Gaussian, sigmoid, and tanh activation functions using our non von Neumann 2D CMOS platform is also demonstrated. This process flow shows the feasibility of monolithic and heterogeneous integration of wafer scale 2D materials.

## Hardware Acceleration of Bayesian Network based on Two-dimensional Memtransistors

Y. Zheng, H. Ravichandran, T.F. Schranghamer, N. Trainor, J.M. Redwing, and S. Das

Before Bayes theorem, a renowned analysis method on conditional probability proposed by Thomas Bayes in 18<sup>th</sup> century, natural species have already adopted Bayesian inference as a method to ensure high survivability. The fact that natural species should make critical decisions on forage and reproduction while avoiding predators based on information from sensory organs with limited sensitivity under noisy environment, emphasizes significance of probabilistic computing for evolutionary success. While anatomy of neural hardware with probabilistic computing capability is not fully understood, it is clear that stochastic computing is fundamental for natural intelligence: Bayesian networks (BNs) are of powerful mathematical architecture to reveal details of probabilistic computing. BNs application widely exists in real-life probabilistic problems including medical diagnosis, weather forecasting, computer vision, etc. Meanwhile, there are limited hardware realization of BNs. CMOS-based [1, 2] BNs requires large number of transistors, while memristors [3-5] and spintronics [6-8] requires CMOS peripheral circuits, which limits area and energy efficiency [9]. Here, we overcome these challenges by introducing a BN architecture with compact design and low-power consumption based on 2D memtransistors.

### Reference:

- [1] S. C. Smithson, N. Onizawa, B. H. Meyer, W. J. Gross, and T. Hanyu, "Efficient CMOS Invertible Logic Using Stochastic Computing," *IEEE Transactions on Circuits and Systems I: Regular Papers*, vol. 66, no. 6, pp. 2263-2274, 2019, doi: 10.1109/TCSI.2018.2889732.
- [2] A. Ardakani, F. Leduc-Primeau, N. Onizawa, T. Hanyu, and W. J. Gross, "VLSI Implementation of Deep Neural Network Using Integral Stochastic Computing," *IEEE Transactions on Very Large Scale Integration (VLSI) Systems*, vol. 25, no. 10, pp. 2688-2699, 2017, doi: 10.1109/TVLSI.2017.2654298.
- [3] S. Gaba, P. Knag, Z. Zhang, and W. Lu, "Memristive devices for stochastic computing," in *2014 IEEE International Symposium on Circuits and Systems (ISCAS)*, 1-5 June 2014 2014, pp. 2592-2595, doi: 10.1109/ISCAS.2014.6865703.
- [4] S. Gaba, P. Sheridan, J. Zhou, S. Choi, and W. Lu, "Stochastic memristive devices for computing and neuromorphic applications," *Nanoscale*, 10.1039/C3NR01176C vol. 5, no. 13, pp. 5872-5878, 2013, doi: 10.1039/C3NR01176C.
- [5] P. Knag, W. Lu, and Z. Zhang, "A Native Stochastic Computing Architecture Enabled by Memristors," *IEEE Transactions on Nanotechnology*, vol. 13, no. 2, pp. 283-293, 2014, doi: 10.1109/TNANO.2014.2300342.
- [6] G. Finocchio, M. Di Ventra, K. Y. Camsari, K. Everschor-Sitte, P. Khalili Amiri, and Z. Zeng, "The promise of spintronics for unconventional computing," *Journal of Magnetism and Magnetic Materials*, vol. 521, p. 167506, 2021/03/01/ 2021, doi: <https://doi.org/10.1016/j.jmmm.2020.167506>.
- [7] J. Hu, B. Li, C. Ma, D. Lilja, and S. J. Koester, "Spin-Hall-Effect-Based Stochastic Number Generator for Parallel Stochastic Computing," *IEEE Transactions on Electron Devices*, vol. 66, no. 8, pp. 3620-3627, 2019, doi: 10.1109/TED.2019.2920401.
- [8] R. Venkatesan, S. Venkataramani, X. Fong, K. Roy, and A. Raghunathan, "Spintastic: Spin-based stochastic logic for energy-efficient computing," *2015 Design, Automation & Test in Europe Conference & Exhibition (DATE)*, pp. 1575-1578, 2015.

- [9] K. Yang, D. Fick, M. B. Henry, Y. Lee, D. Blaauw, and D. Sylvester, "16.3 A 23Mb/s 23pJ/b fully synthesized true-random-number generator in 28nm and 65nm CMOS," in *2014 IEEE International Solid-State Circuits Conference Digest of Technical Papers (ISSCC)*, 9-13 Feb. 2014 2014, pp. 280-281, doi: 10.1109/ISSCC.2014.6757434.

## **Identifying Mechanisms for Eliminating Defects during the Laser Welding of Aluminum Alloys**

*A. Saha<sup>1</sup>, J. Rodelas<sup>2</sup>, M. Maguire<sup>3</sup>, T. DebRoy<sup>3</sup>, T. A. Palmer<sup>1</sup>*

*<sup>1</sup> Department of Engineering Science and Mechanics, The Pennsylvania State University*

*<sup>2</sup> Sandia National Laboratory*

*<sup>3</sup> Department of Materials Science and Engineering, The Pennsylvania State University*

Laser welding of high-strength aluminum alloys is limited by the formation of defects like porosity and hot cracking. Vapor cavities, called keyhole, formed due to the high energy density of the laser are inherently unstable due to temperature gradient, vapor recoil pressure, and surface tension, resulting in keyhole-induced porosity. To mitigate these weld defects by varying the weld pool geometry and fluid flow, beam oscillation technique was employed in the laser welding of AA6160 and AA4047 aluminum alloy plates with different amplitudes and frequencies. The effect of circular beam oscillation with high energy density laser on weld pool depth and keyhole-induced porosity has been studied. An inverse relation between weld depth and oscillation frequency was observed due to the heat distribution and the highest frequency weld showed the lowest depth with respect to the non-oscillation weld pool. The porosity was reduced when the oscillation frequency was increased but at 300Hz frequency, a sudden dip in the pore volume fraction was observed. According to the pore morphology analysis, the smaller pores are spherical with high sphericity and aspect ratio, whereas the larger pores are elongated in shape with low sphericity and aspect ratio. In the higher amplitude welds, pores are localized at the bottom of the weld pool. On the other hand, pores in the lower amplitude welds are present throughout the weld pool depth. This study shows that beam oscillation during laser welding can be used as a tool to control the morphology and distribution of weld defects.

# Drawn-on-Skin Bioelectronics for Motion Artifact-Free Sensing and Point-of-Care Treatment

Faheem Ershad<sup>1</sup> and Cunjiang Yu<sup>1,2\*</sup>

<sup>1</sup>Department of Biomedical Engineering, Pennsylvania State University, State College, PA

<sup>2</sup>Department of Engineering Science and Mechanics, Pennsylvania State University, State College, PA

**Introduction:** Extraction of physiological and physical signals from human skin for health monitoring, disease prevention, and treatment is critical to sustain the wellbeing of humans. Recent advances in wearable bioelectronics which attach directly to the epidermal surface have suggested certain pathways. However, the existing wearable bioelectronics are susceptible to motion artifacts as they lack proper adhesion and conformal interfacing with the skin during motion. Here, we present ultra-conformal Drawn-on-Skin (DoS) electronics as a new bioelectronics platform for on-demand multifunctional, motion artifact-free sensing. DoS bioelectronics is created by liquid functional inks drawn into stencils using ballpoint pens directly on human skin. Upon drawing, an ultra-conformal, robust, and stretchable interface that is immune to motion is formed between DoS electronics and skin. This platform resolves the long-standing challenge of motion artifacts, without the need for additional hardware or computation.

**Materials and Methods:** The DoS devices are based on the Ag flakes/poly(3,4-ethylenedioxythiophene)-poly(styrenesulfonate) (Ag-PEDOT:PSS) composite, poly(3-hexylthiophene-2,5-diyl) nanofibrils (P3HT-NF), and ion gel as the conductive, semiconducting, and dielectric inks, respectively. The ink drawing characteristics, mechanical properties, skin compatibility, and electrical performances of the inks were evaluated. Devices such as transistors, heaters, strain, temperature, hydration, and electrophysiological (EP) sensors were developed (**Fig. 1a**) and characterized. The DoS EP sensors were compared to gel and mesh electrodes for their performance under motion during EP sensing. DoS electronics based electrical stimulation using a mouse model was performed to show accelerated wound healing.

**Results and Discussion:** The DoS inks can be easily drawn with sufficient resolution (~300  $\mu\text{m}$  line width), are mechanically stretchable up to 30%, do not cause any inflammatory response for up to 48 hrs according to histological studies, and have good electrical characteristics (conductive ink: 1.2  $\Omega/\text{sq}$ ) even under mechanical deformation. The signal-to-noise (SNR) ratios of the ECG signal perturbed by skin deformation (**Fig. 1b**) were 50, 20, and 12 dB for the DoS EP, gel, and mesh electrodes, respectively. Furthermore, the spectrogram showed that electromyogram (EMG) signal (<250 Hz) was not contaminated (**Fig. 1c**) by skin vibration when using the DoS EP sensors, unlike the others. In the wound healing experiment, electrical stimulation applied through custom DoS electrodes closed a skin wound about twice as fast as the control.

**Conclusion:** The inks, pens, and stencils serve as a toolkit for easy construction of customizable DoS devices and sensors, which are robust against motion artifacts. With further optimization of functional ink materials, sensor/device constructions and performances, studies of the sensor/device variability, and implementation of additional functionalities, DoS electronics can be implemented as a new, simple, and easily accessible yet promising personalized bioelectronics and healthcare tool.

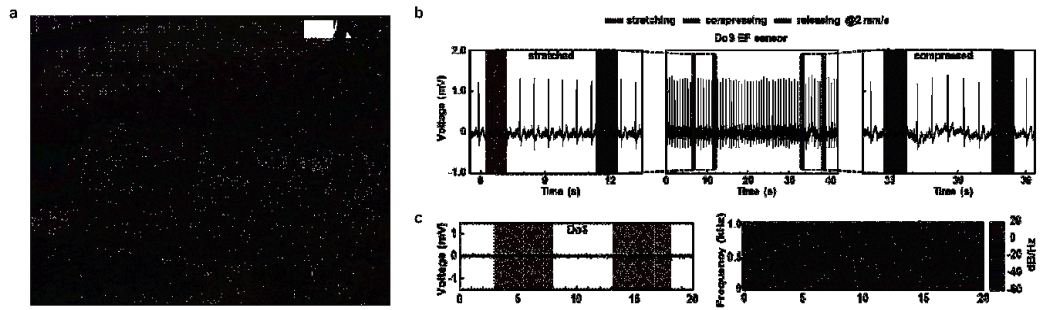
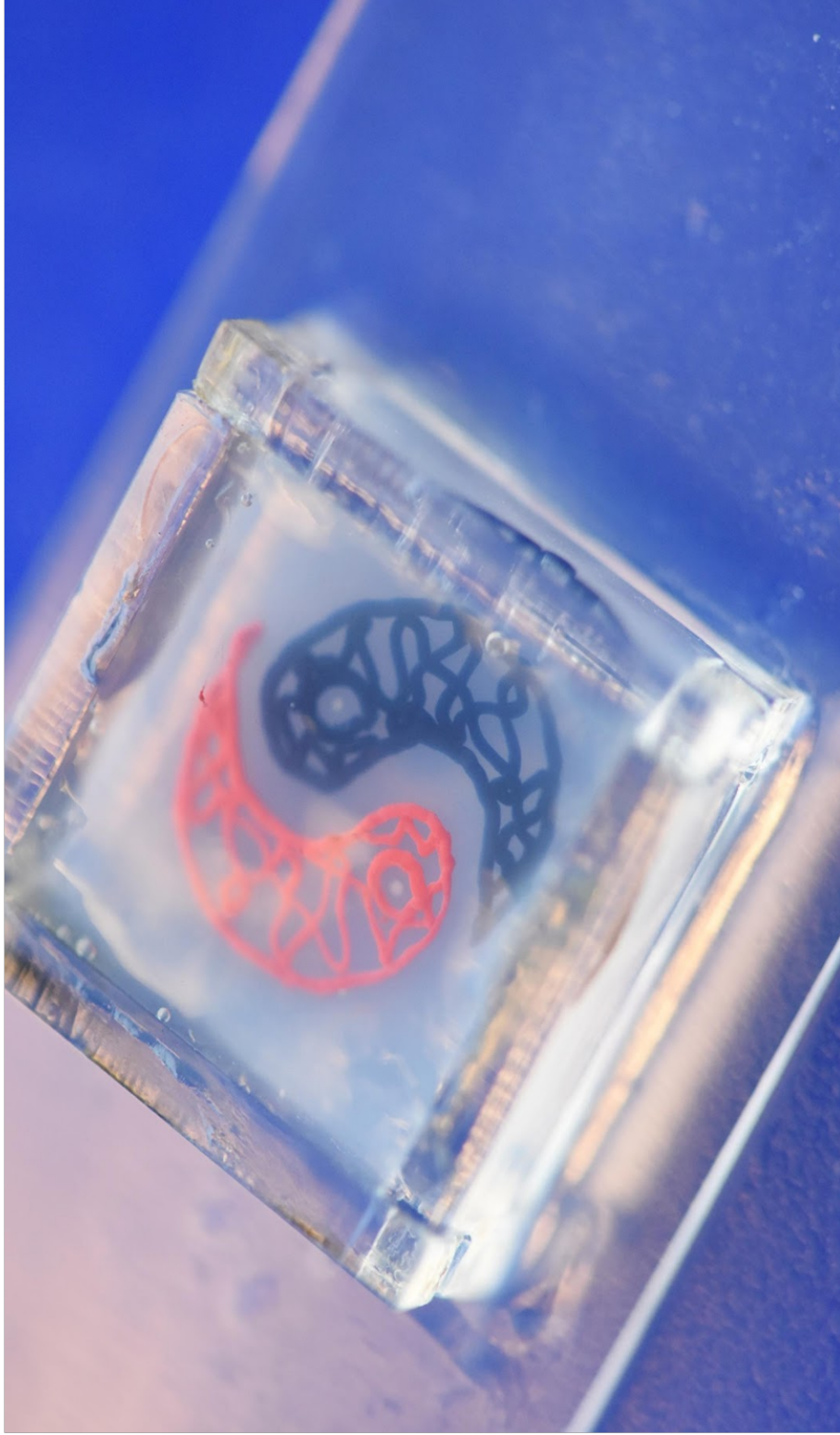


**Figure 1.** DoS electronics. a) Various DoS devices and sensors that can be fabricated on skin. b) ECG signals show no change in the waveform during various deformations. c) Vibrating the skin (pink sections) does not affect the EMG potentials in the time and time-frequency domains.

# Art-in-Science

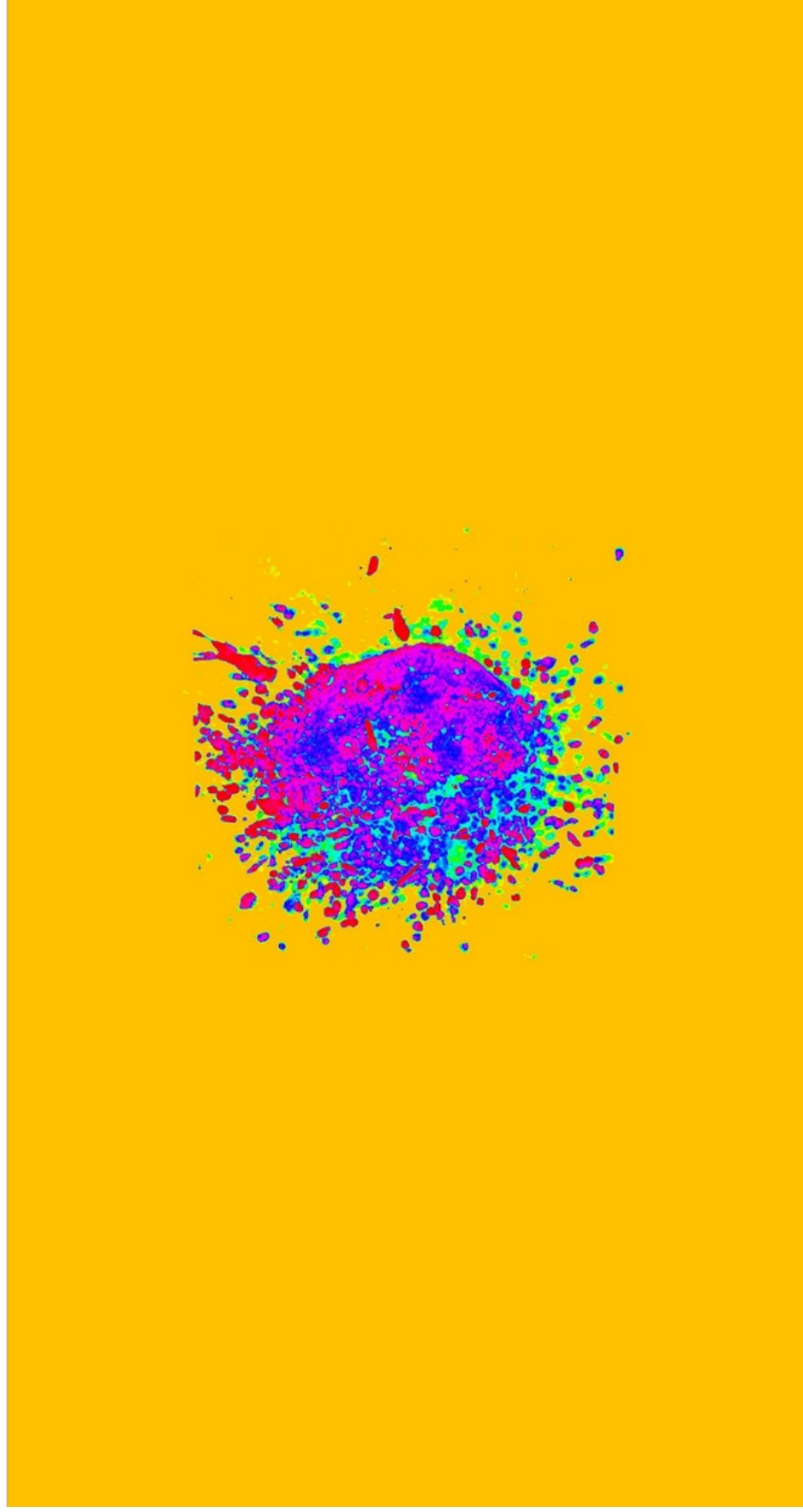
**“Balance”**  
Altan Alioğlu, Advised by Dr. Ibrahim Ozbolat



To demonstrate 3D bioprinting capabilities, a vascular network with Ying and Yang design printed inside a transparent support bath. Two spheroid cell clusters are placed at the centers.

## “Breast Cancer Spheroid”

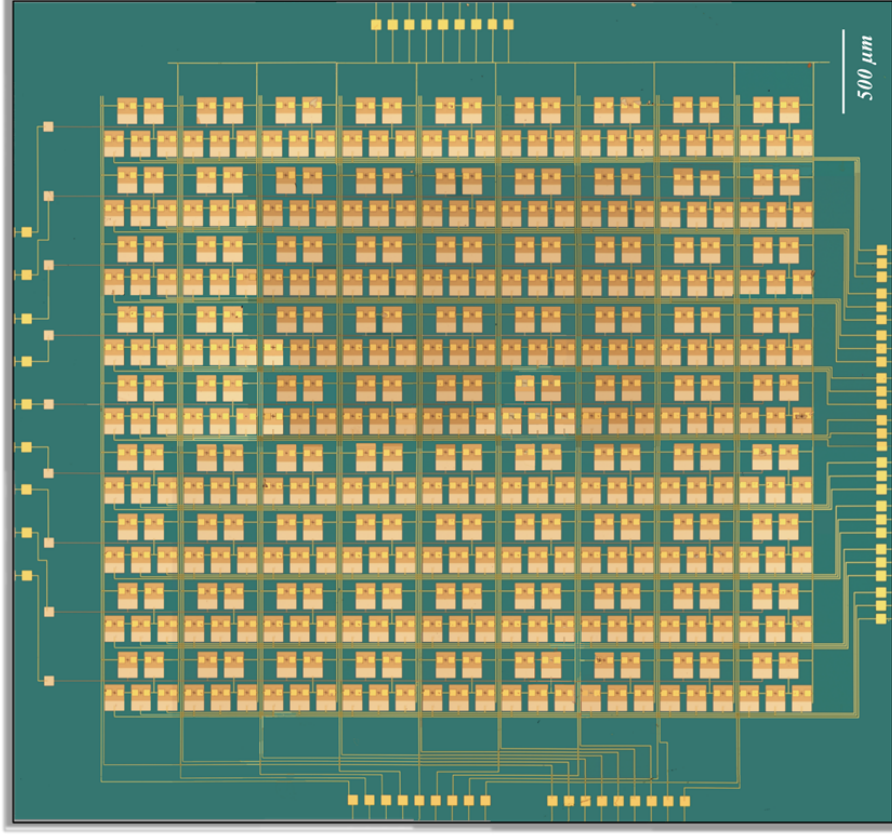
Momoka Nagamine, Advised by Dr. Ibrahim  
Ozbolat



3D reconstruction image of a metastatic breast cancer spheroid taken by a multiphoton microscope. These breast cancer spheroids are used to generate in vitro breast cancer models using bioprinting technologies.

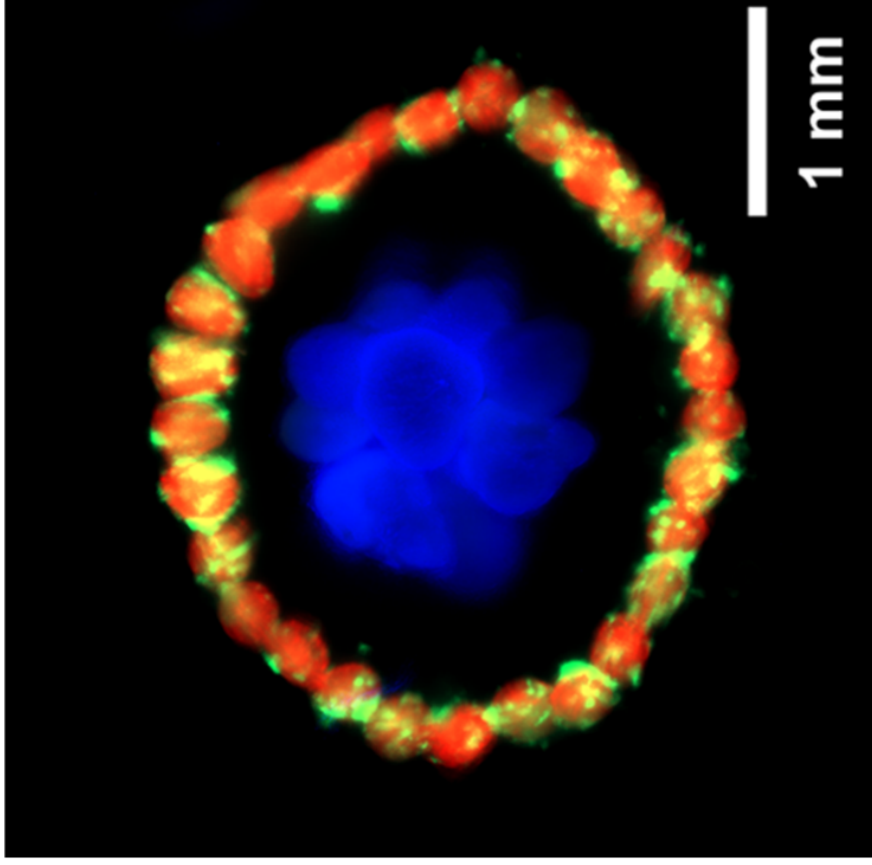
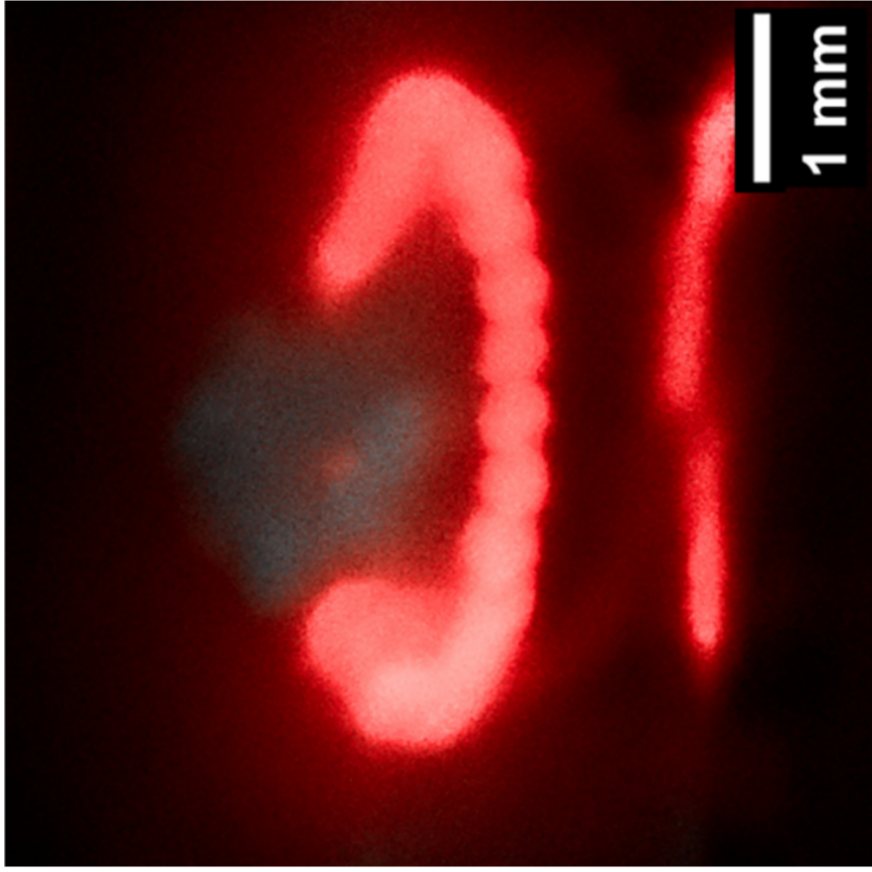
## “Secure Communication using Monolayer MoS<sub>2</sub>”

Akhil Dodda, Advised by Dr. Saptarshi Das



*Optical image of the medium scale integrated chip based on monolayer MoS<sub>2</sub> FETs for image encryption. Each transistor cell is locally back-gated using a gate-dielectric stack comprising of atomic layer deposition (ALD) grown 50 nm Al<sub>2</sub>O<sub>3</sub> on sputter-deposited 50/20 nm Pt/TiN to accomplish sensing and encoding functionalities. All the back-gate islands were placed on a commercially purchased SiO<sub>2</sub>/p<sup>++</sup>-Si substrate. The entire hardware platform utilizes a total of 405 MoS<sub>2</sub> FETs to encrypt the 9 × 9-pixel images for secure communication.*

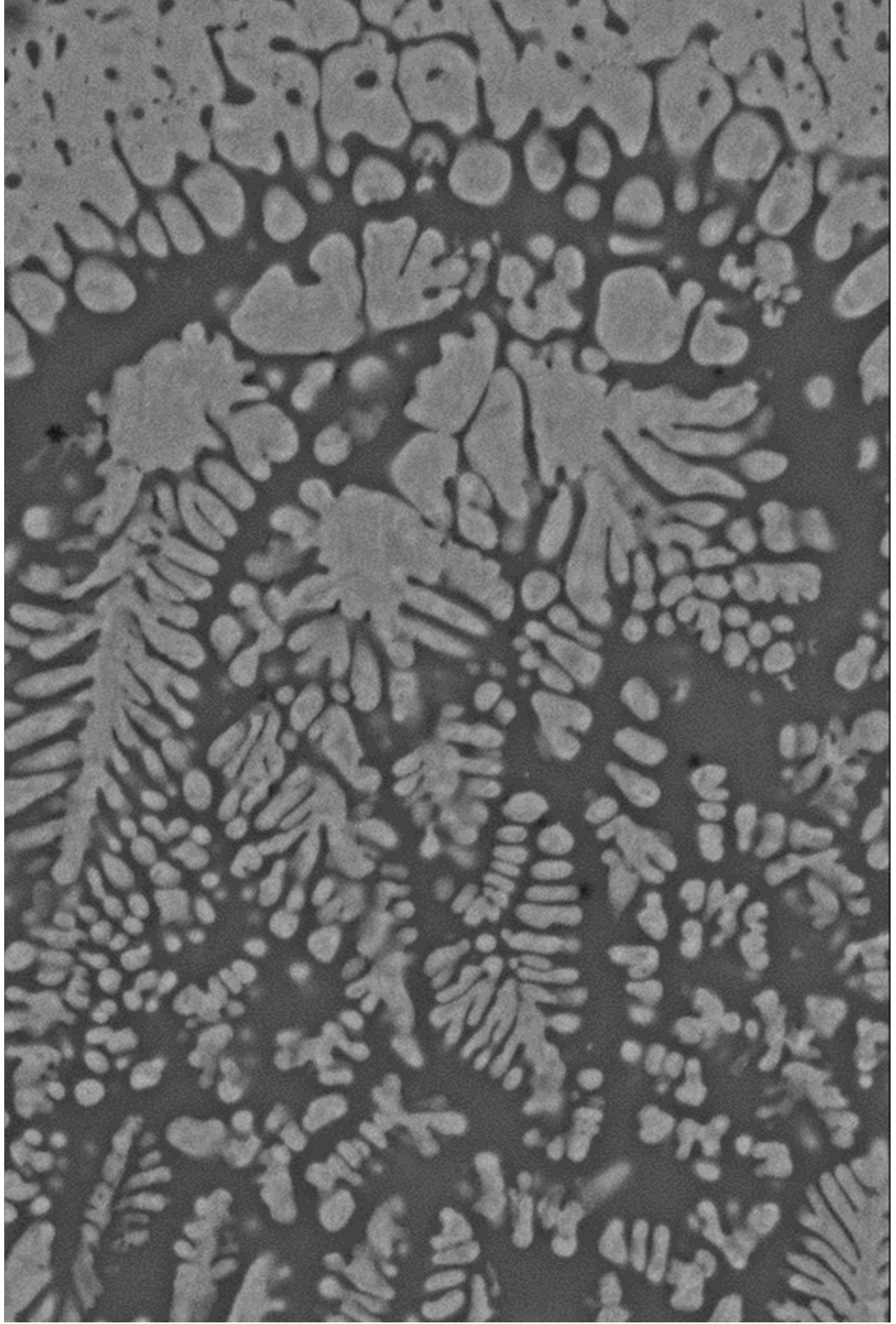
**“Saturn with Planetary Ring System”**  
Myoung Hwan Kim, Advised by Dr. Ibrahim  
Ozbolat



Saturn and its planetary ring system was three-dimensionally created with precisely patterned three different cell types (Red: human umbilical vein endothelial cells, Green: MDA-MB-231, and Blue: human bone marrow-derived mesenchymal stem cells) using aspiration assisted freeform bioprinting system.

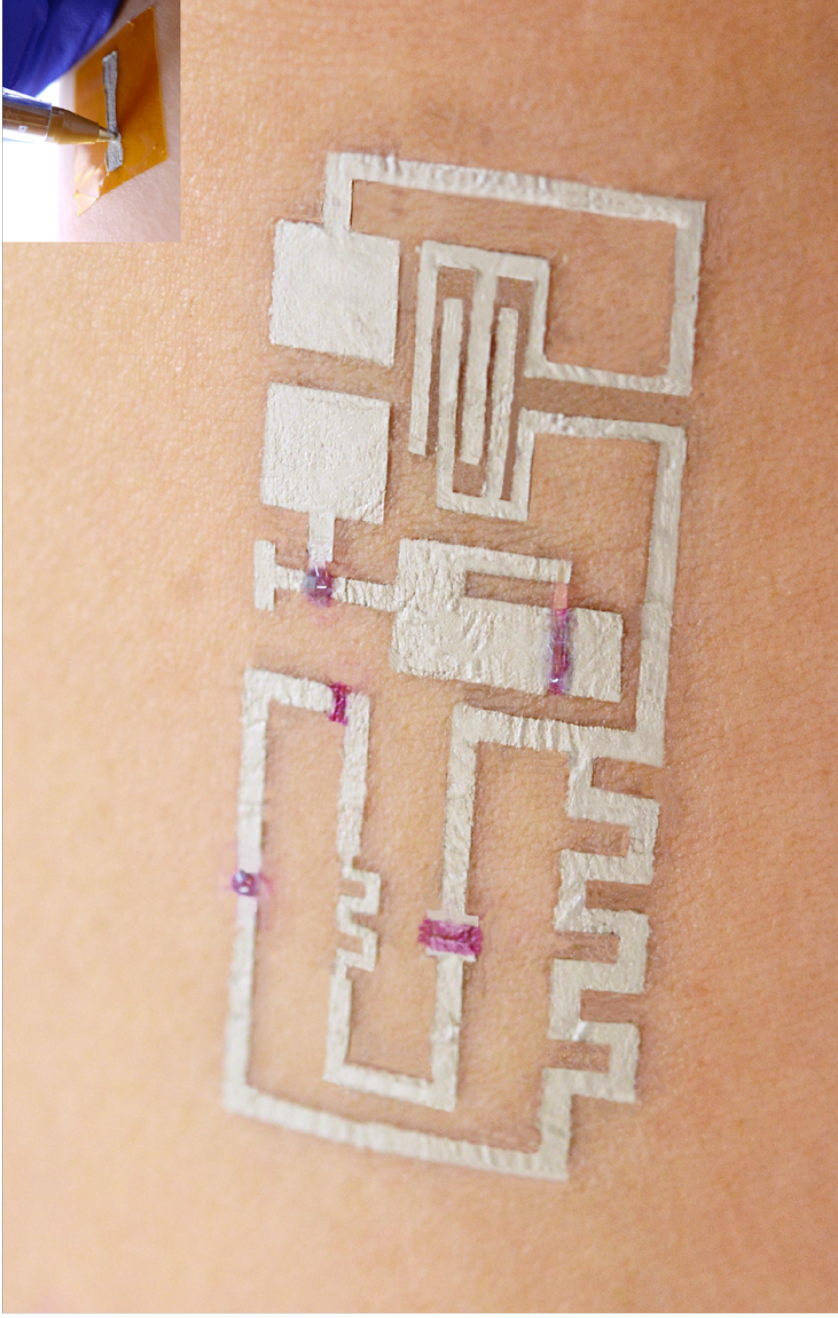
## “Dendritic solidification in Nickel Titanium Alloy”

Arnab Chatterjee



## “Drawn-on-Skin Bioelectronics”

Faheem Ershad, Advised by Dr. Ibrahim Ozbolat



Here, we present Drawn-on-Skin (DoS) electronics as a new bioelectronics platform for multifunctional, motion artifact-free sensing. DoS bioelectronics is created by liquid functional inks drawn into stencils using ballpoint pens directly on human skin. Upon drawing, an ultra-conformal, robust, and stretchable interface that is immune to motion is formed between DoS electronics and skin. This platform resolves the long-standing challenge in the wearable bioelectronics field of motion artifacts at the skin-electronics interface, without the need for additional hardware or computation. The image here shows a prototype multifunctional integrated system consisting of the DoS transistors, resistors, heaters, and strain, temperature, hydration, and electro-physiological sensors.

## “A Micro-forest in a Nanofilm”

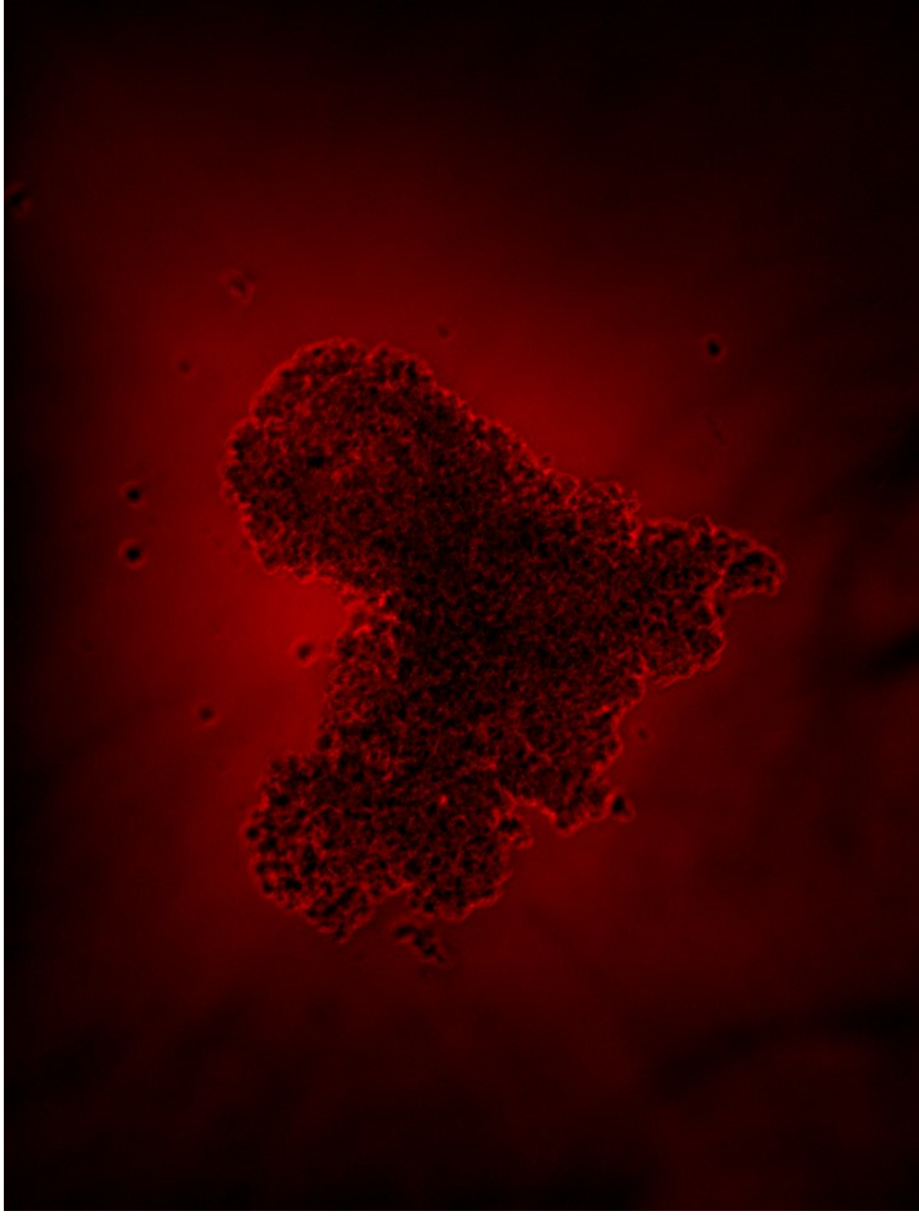
Rahul Pendurthi, Advised by Dr. Saptarshi Das



Dark field image of a transferred monolayer  $\text{MoS}_2$  film on a delaminated PMMA surface. The “roots” are micro-wrinkles in the film, while the forest floor is generated by the undulations on the PMMA surface.

## “LOVE STARTS AT THE CELLULAR LEVEL”

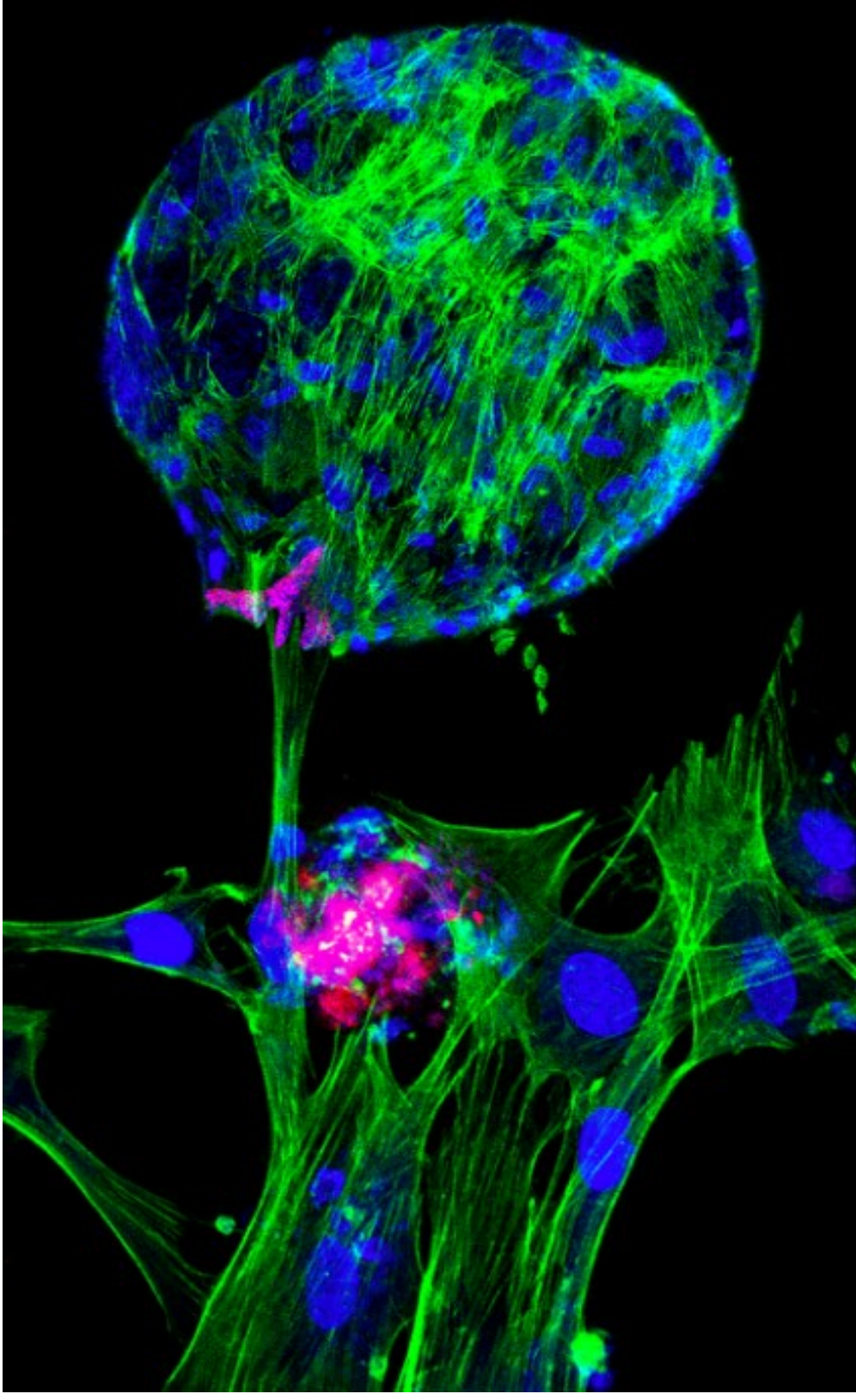
Luis Rivas, Advised BY Dr. Ibrahim Ozbolat



An ImageJ Fiji software figure of human lung fibroblast cells that were stained with fluorescent protein for a live-dead study. These cells were aggregated by Acoustic Levitation at 40kHz using ultrasonic transducers; unexpectedly expressing the shape of a heart.

## THE FIRST CONNECTION of CELL DIMENSIONS

Nazmiye Celik, Advised by Dr. Ibrahim Ozbolat



3D Rat Muscle-derived progenitor cells (MPCs) are communicating with 2D Rat Adipose-derived stem cells (ADSCs) Cytoskeleton (green) - and cell nuclei (blue) - and bone marker (red)-stained samples were imaged by using a Zeiss LSM 880 Airyscan confocal microscope via ZEN 2.3 SP1 software as 3D z-stack.